LiDAR Remote Sensing Data Collection:
Columbia River Survey
Delivery 11

September 3rd , 2010

Submitted to:

Jacob MacDonald
U.S. Army Corps of Engineers
Portland District
P.O. Box 2946
Portland, OR 97208

Submitted by:

Watershed Sciences
517 SW 2nd Street, Suite 400
Corvallis, OR 97333

529 SW 3rd Ave. Suite 300
Portland, OR 97204

WatershedSciences

LiDAR Remote Sensing Data Collection:

Columbia River Survey

Delivery 11

TABLE OF CONTENTS

1. Overview 1

2. Acquisition 3
   2.1 Airborne Survey – Instrumentation and Methods 3
   2.2 Ground Survey – Instrumentation and Methods 4
      2.2.1 Survey Control 4
      2.2.2 RTK Survey 8
   3. LiDAR Data Processing 10
   3.1 Applications and Work Flow Overview 10
   3.2 Aircraft Kinematic GPS and IMU Data 11
   3.3 Laser Point Processing 11

4. LiDAR Accuracy Assessment 12
   4.1 Laser Noise and Relative Accuracy 12
   4.2 Absolute Accuracy 13

5. Study Area Results 14
   5.1 Data Summary 14
   5.2 Data Density/Resolution 14
   5.3 Relative Accuracy Calibration Results 40
   5.4 Absolute Accuracy 43

6. Breakline Enforced Terrain Model 44

7. Projection/Datum and Units 45

8. Deliverables 45

9. Selected Images 46

10. Glossary 58

11. Citations 59

Appendix A 60

Appendix B 62

1. Overview

Watershed Sciences, Inc. (WS) collected Light Detection and Ranging (LiDAR) data of the Columbia River in Oregon, Washington, Idaho, and Montana. The requested AOI area for this delivery was 206,986 acres. The area was expanded to include a 100m buffer to ensure complete coverage and adequate point densities around survey area boundaries, resulting in 215,077 acres of delivered data. LiDAR data for Delivery 11 was collected between April 23rd and May 6th, 2010 (**Figure 1**). This area includes Flathead River from the south end of Flathead Lake to the Hungry Horse Dam in Montana. This report contains maps and information specific to Delivery 11, but has been appended to the previous delivered reports to generate a cumulative data summary for UTM Zone 10 and 11. Accuracy and density data will continue to be updated as additional data is processed.

Figure 1. Columbia River survey delivery status overview.

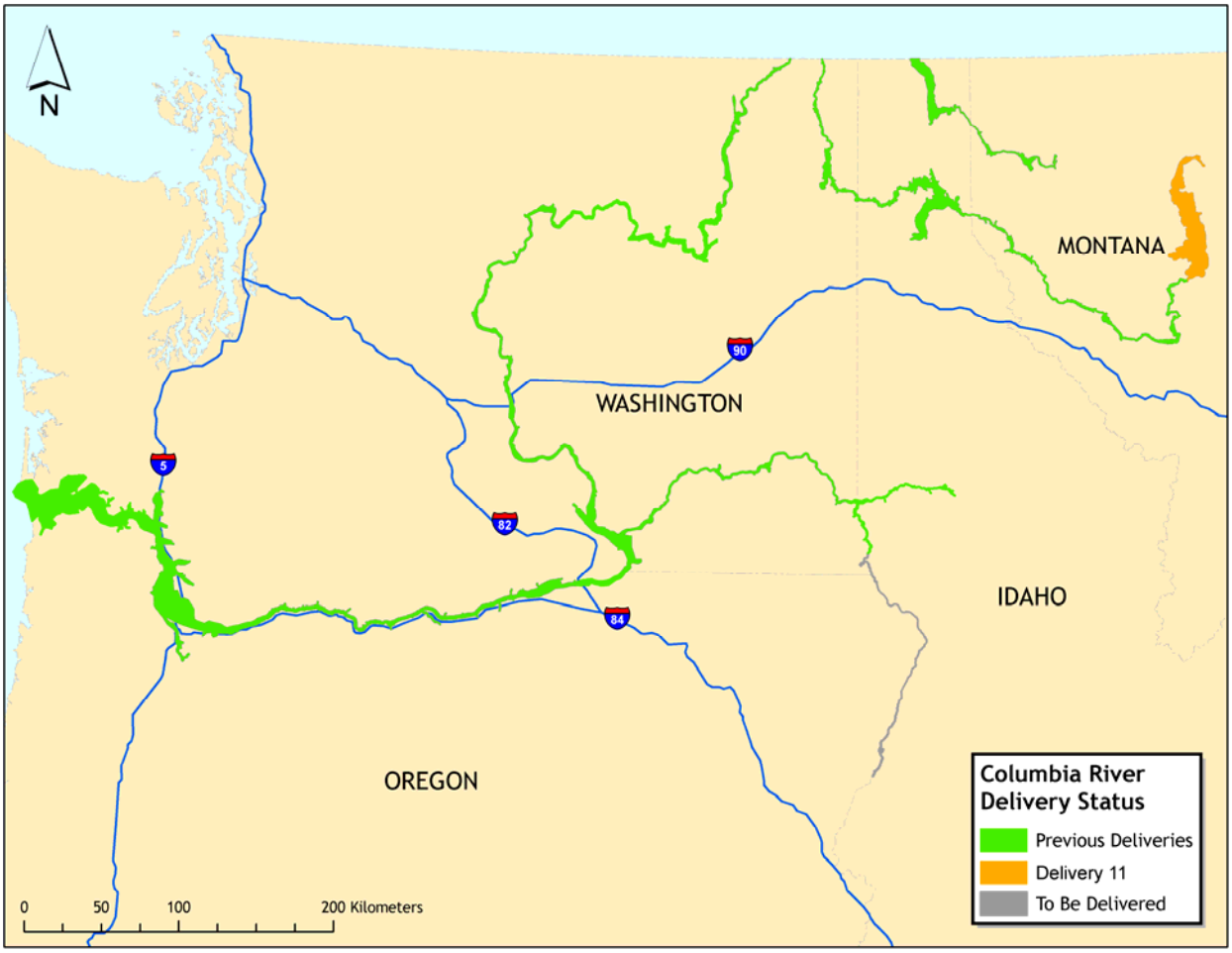

Table 1. Columbia River, UTM Zone 10 and 11 LiDAR deliveries to date.

UTM 10 Delivery	Date	Total Acres Flown	AOI Acres
1	April 15, 2010	129,000	125,409
2	May 13, 2010	191,071	181,694
4	June 8, 2010	324,600	314,797
8	July 22, 2010	104,774	94,054
UTM 11 Delivery	**Date**	**Total Acres Flown**	**AOI Acres**
1	April 15, 2010	206,500	187,764
3	May 20, 2010	115,200	102,837
5	June 17, 2010	52,785	44,273
6	June 23, 2010	99,741	89,405
6b	July 1, 2010	67,729	60,369
7	July 16, 2010	187,130	170,290
8	July 22, 2010	55,374	51,985
9	July 29, 2010	115,148	103,574
10	August 11, 2010	73,376	61,890
11	September 3, 2010	215,077	206,986

2. Acquisition

2.1 Airborne Survey – Instrumentation and Methods

The LiDAR survey uses Leica ALS50 Phase II and ALS60 laser systems. For the Columbia River survey sites, the sensor scan angle was ±14° from nadir[1] with a pulse rate designed to yield an average native density (number of pulses emitted by the laser system) of ≥ 8 points per square meter over terrestrial surfaces. It is not uncommon for some types of surfaces (e.g. dense vegetation or water) to return fewer pulses than the laser originally emitted. These discrepancies between 'native' and 'delivered' density will vary depending on terrain, land cover and the prevalence of water bodies.

The Cessna Caravan is a stable platform, ideal for flying slow and low for high density projects. The Leica ALS60 sensor head installed in the Caravan is shown on the left.

All areas were surveyed with an opposing flight line side-lap of ≥60% (≥100% overlap) to reduce laser shadowing and increase surface laser painting. The Leica laser systems allow up to four range measurements (returns) per pulse, and all discernable laser returns were processed for the output dataset.

To accurately solve for laser point position (geographic coordinates x, y, z), the positional coordinates of the airborne sensor and the attitude of the aircraft were recorded continuously throughout the LiDAR data collection mission. Aircraft position was measured twice per second (2 Hz) by an onboard differential GPS unit. Aircraft attitude was measured 200 times per second (200 Hz) as pitch, roll and yaw (heading) from an onboard inertial measurement unit (IMU). To allow for post-processing correction and calibration, aircraft/sensor position and attitude data are indexed by GPS time.

[1] Nadir refers to the perpendicular vector to the ground directly below the aircraft. Nadir is commonly used to measure the angle from the vector and is referred to a "degrees from nadir".

2.2 Ground Survey – Instrumentation and Methods

Trimble GPS survey equipment

The following ground survey data were collected to enable the geo-spatial correction of the aircraft positional coordinate data collected throughout the flight, and to allow for quality assurance checks on final LiDAR data products.

2.2.1 Survey Control

Simultaneous with the airborne data collection mission, we conducted multiple static (1 Hz recording frequency) ground surveys over monuments with known coordinates (**Table 2**). Survey control monuments were occupied by a Trimble GPS base station for an initial period of at least eight hours. All monuments were occupied during a subsequent second session with an observation period of at least four hours. Additional occupations were conducted as necessary. GPS measurements were made with dual frequency L1-L2 receivers with carrier-phase correction.

Watershed Sciences established monuments using aluminum survey caps provided by the Army Corps of Engineers. Monuments were placed using 5/8" by 30" rebar covered with a 2" top aluminum cap stamped "U.S. Army C. of E. Portland Dist.". In addition, monuments were stamped in the field with the year and monument ID number.

As an initial check, the NGS on-line positioning user service (OPUS), was used to generate a corrected position for all base station observations. OPUS provides a measurement solution based on three surrounding continuously operating reference stations (CORS). OPUS output includes a solution report with positional accuracy confidence intervals for adjusted coordinates and elevations. The solution report is one component in assessing the quality of the OPUS GPS measurement solutions. Statistical checks of GPS base station positions and repeat control observations include the OPUS solution extended output report. In addition, the standard deviation, kurtosis, and skew of the measurement distribution for each base station occupation were compared. Longitude, latitude, and elevation distributions were separated, and graphic distributions of the positions were plotted for consistency.

Indexed by time, these GPS data are used to correct the continuous onboard measurements of aircraft position recorded throughout the mission. Control monuments were located within 13 nautical miles of the survey area(s).

David Evans and Associates (DEA) provided the official quality assurance and control checks of all monuments in the Columbia River project. DEA provided official coordinates for each monument through the OPUS online datasheet publication tool located on the USGS website. All monuments established by Watershed Sciences were published and made publicly available by DEA on the OPUS online datasheet website.

Table 2. DEA Certified Survey Control coordinates for Columbia River, UTM Zones 10 and 11.

Base Station ID	Datum: NAD83 (CORS96)		GRS80
	Latitude	Longitude	Ellipsoid Z (m)
1001-02	48 23 56.98482	115 34 50.21483	616.831
1001-04	48 32 51.20358	115 57 51.74806	548.385
1001-05	48 48 13.76901	116 19 54.78221	668.822
1001-06	48 44 31.95802	116 16 27.48836	696.109
1001-08	46 30 08.41845	116 25 47.09675	418.636
1001-09	46 29 22.56717	116 36 33.78201	660.133
1001-10	46 26 48.57603	116 49 22.85153	242.283
1001-11	46 25 37.24185	116 59 37.84845	209.654
1001-12	46 25 28.18217	117 02 53.46337	217.828
1001-14	46 31 44.00816	117 17 42.94603	806.850
1001-15	46 09 54.03858	117 05 33.99519	976.572
1001-16	46 17 49.31959	117 02 40.71052	630.840
1001-17	46 37 03.17427	117 24 34.40297	712.061
1001-18	46 33 18.67588	118 02 38.51875	431.742
1001-19	46 33 41.76244	117 53 55.49244	401.264
1001-25	46 15 24.33299	119 06 44.28022	99.580
1001-26	46 04 58.38585	118 54 08.97171	95.397
1001-27	46 32 46.94111	118 32 25.89962	226.994
1001-29	45 56 24.58774	119 18 39.87547	74.982
1001-30	45 53 42.93963	119 30 34.66550	68.346
1001-31	46 19 13.63661	118 45 33.52351	144.348
1001-32	46 26 46.23824	119 14 59.85289	171.387
1001-33	46 35 03.15570	119 17 48.43777	264.490
1001-34	46 42 39.57396	119 57 04.04702	132.138
1001-35	46 54 34.61756	119 56 52.68161	245.487
1001-36	46 38 32.50510	119 44 38.56540	107.820
1001-38	47 31 01.69423	120 17 43.85407	205.566
1001-39	47 43 16.43454	120 12 05.54248	279.646
1001-40	47 39 26.74447	120 12 51.23753	201.909
1001-41	47 52 34.16625	119 55 30.35960	359.683
1001-42	48 39 42.07553	117 23 30.60187	622.832
1001-43	48 51 35.80852	117 22 12.13785	626.785
1001-44	48 20 17.00710	117 17 38.10574	609.766
1001-45	48 04 42.09424	115 58 11.36504	684.158
1001-46	47 53 57.17442	115 40 38.25177	749.758

Base Station ID	Datum: NAD83 (CORS96)		GRS80
	Latitude	Longitude	Ellipsoid Z (m)
1001-49	46 09 55.00289	123 08 46.34550	-15.171
1001-50	45 40 13.04473	122 45 28.31957	-14.798
1001-51	45 32 52.95214	122 24 43.61919	-13.122
1001-52	45 41 51.83136	122 44 01.68085	-14.212
1001-53	45 35 59.70787	122 37 05.21497	-9.882
1001-54	45 27 24.11550	122 33 34.92185	180.288
1001-55	45 53 58.62988	122 47 51.37726	-13.396
1001-56	45 51 15.81779	122 42 09.46590	52.603
1001-57	46 02 26.42971	122 52 01.38200	-14.220
1001-58	46 06 32.94910	122 53 01.76755	-13.834
1001-59	47 54 08.17176	118 20 03.21717	391.203
1001-60	48 11 09.36642	117 01 49.51670	610.614
1001-62	48 07 48.72502	119 18 57.73566	348.902
1001-63	48 01 58.81548	118 57 40.44020	313.960
1001-64	48 07 07.96832	118 13 10.22406	462.187
1001-65	47 55 43.85009	118 41 20.44432	376.281
1001-66	47 52 22.12504	118 19 29.21408	543.652
1001-67	48 01 32.65643	119 34 09.57665	313.446
1001-70	45 54 49.89349	122 48 12.52910	-13.496
1001-71	46 10 44.41058	123 22 37.98798	-16.494
1001-72	46 14 15.72282	123 23 47.41730	-17.845
1001-73	46 21 04.74607	123 36 24.40429	-16.407
1001-74	46 21 11.60474	123 48 45.17118	-10.861
1001-75	46 10 23.59054	123 49 53.71402	-18.456
1001-76	47 52 21.92656	118 19 29.68485	543.446
1001-77	48 05 40.67814	118 13 22.57872	444.409
1001-78	48 15 21.98771	118 08 01.18819	379.954
1001-79	48 26 26.39581	118 10 13.95487	521.192
1001-80	45 42 49.27090	121 30 39.83749	6.517
1001-81	45 40 29.62695	121 15 50.33345	11.637
1001-82	45 38 19.36273	120 58 01.24913	207.447
1001-83	45 43 47.54805	120 39 04.19716	75.569
1001-84	45 42 04.13225	120 20 40.20502	150.893
1001-85	45 47 05.76648	120 02 18.05975	109.677
1001-86	45 50 33.55651	119 42 34.81642	65.288
1001-87	46 11 28.87024	123 45 29.15267	-1.992

Base Station ID	Datum: NAD83 (CORS96)		GRS80
	Latitude	Longitude	Ellipsoid Z (m)
1001-88	46 12 49.68406	123 32 29.63950	-21.069
1001-89	46 12 49.74473	123 32 29.55793	-21.065
1001-90	46 09 11.71519	123 52 41.61197	-19.966
1001-91	46 11 48.84319	118 58 46.57016	99.304
1001-92	48 11 13.44329	116 26 13.31352	614.124
1001-93	48 07 22.89093	116 09 43.76442	617.352
1001-94	48 10 32.72793	116 13 56.37429	614.029
1001-96	48 19 22.29241	116 26 54.84908	626.669
1001-97	48 13 57.90901	116 31 44.49034	618.705
1001-98	48 51 09.21908	117 53 28.28571	466.493
1001-99	48 54 44.63988	117 47 25.87213	396.158
1001-100	48 34 12.52863	118 06 49.31297	376.733
1001-101	48 43 02.83908	118 01 34.25317	392.519
1001-103	48 19 50.72828	114 11 47.13329	913.855
1001-104	48 18 32.50920	114 13 58.76651	887.556
1001-106	48 43 14.07373	116 18 37.83016	681.969
1001-107	47 49 55.98524	115 35 13.49428	706.003
1001-108	47 26 26.50061	114 52 29.24524	736.687
1001-109	47 34 38.93062	115 18 16.78201	727.692
1001-110	47 20 27.83571	114 37 54.76413	763.841
1001-111	47 18 47.09352	114 21 25.31047	753.416
1001-112	47 29 18.70339	114 20 30.58228	825.889
1001-113	48 04 52.09014	114 05 57.68806	888.638
1001-114	47 52 02.68632	114 16 28.44232	870.056
1001-121	47 41 34.65105	114 11 05.77338	879.665
1001-122	47 41 34.16354	114 11 06.37528	879.636
1001-123	48 07 27.25462	114 11 31.97132	869.285
1001-124	48 07 15.01784	114 14 25.37373	873.092
1001-125	48 23 40.92084	115 33 37.77048	615.561
86-19-305	46 11 52.54563	122 54 46.81344	-6.618
AD9155	46 09 32.38751	123 53 12.26752	-20.448
AD9552	46 18 21.26198	119 18 36.67971	100.325
SD0651	46 13 31.35468	124 00 30.58787	-14.296
SU0682	47 50 08.06221	114 20 07.84551	881.843
DH8973	48 18 12.73636	116 33 18.87333	631.363

2.2.2 RTK Survey

To enable assessment of LiDAR data accuracy, ground check points were collected using GPS based real-time kinematic (RTK) surveying. Instrumentation included multiple Trimble DGPS units (R8). RTK surveying allows for precise location measurements with an error (σ) of ≤ 1.5 cm (0.6 in).

For the RTK survey, the ground crew used a roving unit to receive radio-relayed corrected positional coordinates for all ground truth points from a GPS base station set up over certified survey control monuments. **Figure 2**, below, portrays the distribution of RTK points and base station locations used for the current delivery of Columbia River survey areas. RTK points were collected on hard surfaces that were easily distinguishable within the LiDAR dataset. Paved surfaces, including roads, paths, and parking lots, were the primary surface target. After all paved surfaces had been exhausted, hard packed gravel roads became the secondary target for RTK, followed by hard packed dirt roads. Hard surfaces are targeted in areas that are clearly visible (and likely to remain visible) from the sky during data acquisition.

In order to facilitate comparisons with LiDAR data, RTK measurements were not taken on highly reflective surfaces such as center line stripes or lane markings on roads. RTK points were taken no closer than one meter to any nearby terrain breaks such as road edges or drop offs to ensure an accurate comparison between RTK and LiDAR ground data. In addition, attempts were made to collect RTK points on locations that could be readily identified and occupied during subsequent field visits. RTK measurements were collected approximately 1-2 meters from one another to support measurement independence.

An RTK point acquisition period is five seconds long and includes three individual one-second measurements averaged together. The five second observation period ensures that an accurate RTK point was taken. RTK points were not taken during periods when PDOP was greater than three, when less than six satellites were visible, or when horizontal and vertical RMS values were greater than 0.03 m. An RMS value of 0.03 m indicates that an RTK measurement is within 0.03 m of its actual position 68% of the time. An RTK check point was also taken at the beginning and end of each RTK session as close to the base station location as possible to provide an on-the-spot vertical accuracy check.

Figure 2. RTK point and control monument locations used in Delivery 11, UTM 11.

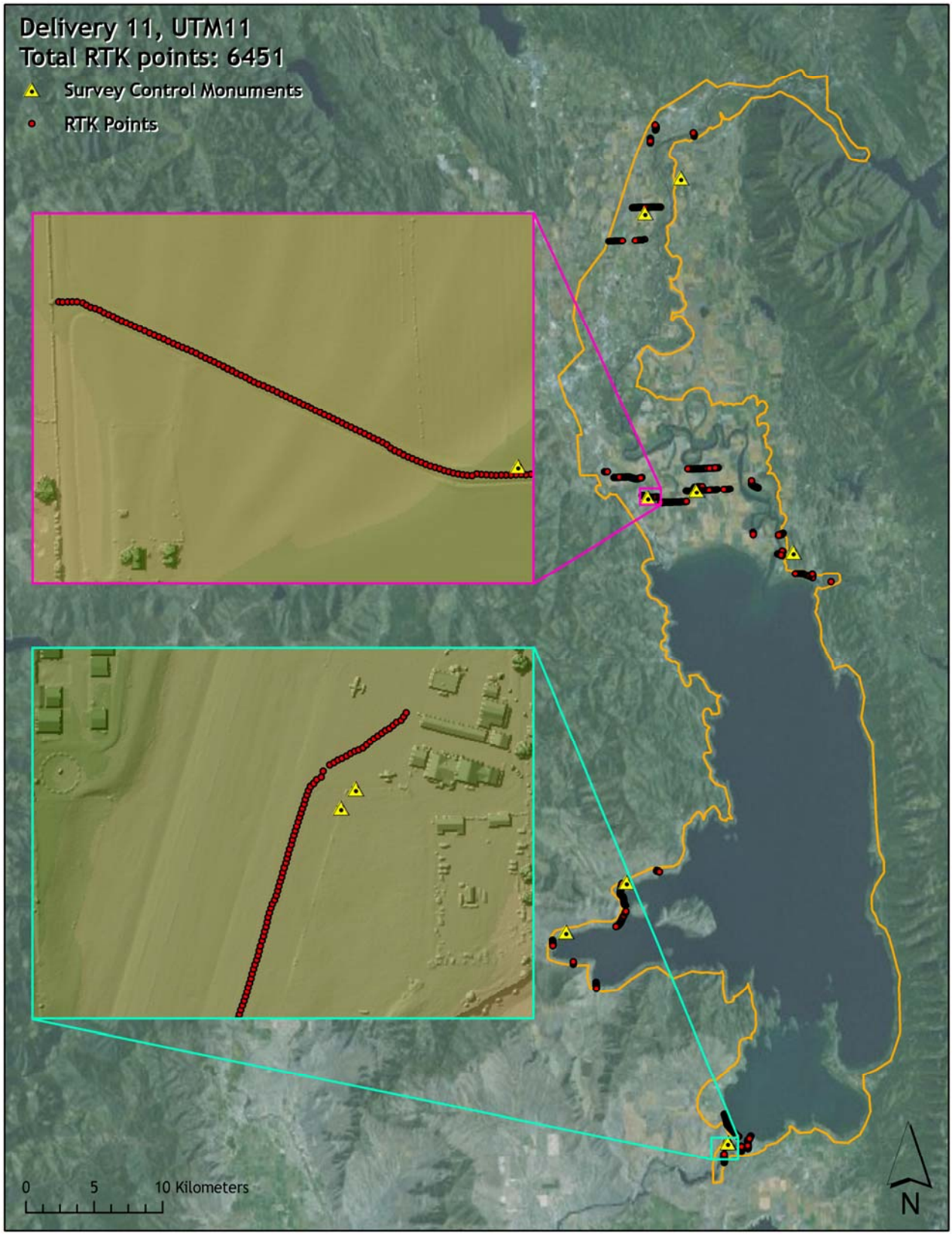

3. LiDAR Data Processing

3.1 Applications and Work Flow Overview

1. Resolved kinematic corrections for aircraft position data using kinematic aircraft GPS and static ground GPS data.

   Software: Waypoint GPS v.8.10, Trimble Geomatics Office v.1.62
2. Developed a smoothed best estimate of trajectory (SBET) file that blends post-processed aircraft position with attitude data. Sensor head position and attitude were calculated throughout the survey. The SBET data were used extensively for laser point processing.

   Software: IPAS v.1.35
3. Calculated laser point position by associating SBET position to each laser point return time, scan angle, intensity, etc. Created raw laser point cloud data for the entire survey in *.las (ASPRS v. 1.2) format.

   Software: ALS Post Processing Software v.2.69
4. Imported raw laser points into manageable blocks (less than 500 MB) to perform manual relative accuracy calibration and filter for pits/birds. Ground points were then classified for individual flight lines (to be used for relative accuracy testing and calibration).

   Software: TerraScan v.10.009
5. Using ground classified points per each flight line, the relative accuracy was tested. Automated line-to-line calibrations were then performed for system attitude parameters (pitch, roll, heading), mirror flex (scale) and GPS/IMU drift. Calibrations were performed on ground classified points from paired flight lines. Every flight line was used for relative accuracy calibration.

   Software: TerraMatch v.10.006
6. Position and attitude data were imported. Resulting data were classified as ground and non-ground points. Statistical absolute accuracy was assessed via direct comparisons of ground classified points to ground RTK survey data. Data were then converted to orthometric elevations (NAVD88) by applying a Geoid09 correction. Ground models were created as a triangulated surface and exported as ArcInfo ASCII grids at a 1 –meter pixel resolution.

   Software: TerraScan v.10.009, ArcMap v. 9.3.1, TerraModeler v.10.004

3.2 Aircraft Kinematic GPS and IMU Data

LiDAR survey datasets were referenced to the 1 Hz static ground GPS data collected over pre-surveyed monuments with known coordinates. While surveying, the aircraft collected 2 Hz kinematic GPS data, and the onboard inertial measurement unit (IMU) collected 200 Hz aircraft attitude data. Waypoint GPS v.8.10 was used to process the kinematic corrections for the aircraft. The static and kinematic GPS data were then post-processed after the survey to obtain an accurate GPS solution and aircraft positions. IPAS v.1.35 was used to develop a trajectory file that includes corrected aircraft position and attitude information. The trajectory data for the entire flight survey session were incorporated into a final smoothed best estimated trajectory (SBET) file that contains accurate and continuous aircraft positions and attitudes.

3.3 Laser Point Processing

Laser point coordinates were computed using the IPAS and ALS Post Processor software suites based on independent data from the LiDAR system (pulse time, scan angle), and aircraft trajectory data (SBET). Laser point returns (first through fourth) were assigned an associated (x, y, z) coordinate along with unique intensity values (0-255). The data were output into large LAS v. 1.2 files; each point maintains the corresponding scan angle, return number (echo), intensity, and x, y, z (easting, northing, and elevation) information.

These initial laser point files were too large for subsequent processing. To facilitate laser point processing, bins (polygons) were created to divide the dataset into manageable sizes (< 500 MB). Flightlines and LiDAR data were then reviewed to ensure complete coverage of the survey area and positional accuracy of the laser points.

Laser point data were imported into processing bins in TerraScan, and manual calibration was performed to assess the system offsets for pitch, roll, heading and scale (mirror flex). Using a geometric relationship developed by Watershed Sciences, each of these offsets was resolved and corrected if necessary.

LiDAR points were then filtered for noise, pits (artificial low points) and birds (true birds as well as erroneously high points) by screening for absolute elevation limits, isolated points and height above ground. Each bin was then manually inspected for remaining pits and birds and spurious points were removed. In a bin containing approximately 7.5-9.0 million points, an average of 50-100 points are typically found to be artificially low or high. Common sources of non-terrestrial returns are clouds, birds, vapor, haze, decks, brush piles, etc.

Internal calibration was refined using TerraMatch. Points from overlapping lines were tested for internal consistency and final adjustments were made for system misalignments (i.e., pitch, roll, heading offsets and scale). Automated sensor attitude and scale corrections yielded 3-5 cm improvements in the relative accuracy. Once system misalignments were corrected, vertical GPS drift was then resolved and removed per flight line, yielding a slight improvement (<1 cm) in relative accuracy.

The TerraScan software suite is designed specifically for classifying near-ground points (Soininen, 2004). The processing sequence began by 'removing' all points that were not 'near' the earth based on geometric constraints used to evaluate multi-return points. The

resulting bare earth (ground) model was visually inspected and additional ground point modeling was performed in site-specific areas to improve ground detail. This manual editing of ground often occurs in areas with known ground modeling deficiencies, such as: bedrock outcrops, cliffs, deeply incised stream banks, and dense vegetation. In some cases, automated ground point classification erroneously included known vegetation (i.e., understory, low/dense shrubs, etc.). These points were manually reclassified as non-grounds. Ground surface rasters were developed from triangulated irregular networks (TINs) of ground points.

4. LiDAR Accuracy Assessment

Our LiDAR quality assurance process uses the data from the real-time kinematic (RTK) ground survey conducted in the survey area. For both the UTM 10 and UTM 11 areas delivered to date, a total of **39,757 RTK** GPS measurements were collected on hard surfaces distributed among multiple flight swaths. To assess absolute accuracy, we compared the location coordinates of these known RTK ground survey points to those calculated for the closest laser points.

4.1 Laser Noise and Relative Accuracy

Laser point absolute accuracy is largely a function of laser noise and relative accuracy. To minimize these contributions to absolute error, we first performed a number of noise filtering and calibration procedures prior to evaluating absolute accuracy.

Laser Noise

For any given target, laser noise is the breadth of the data cloud per laser return (i.e., last, first, etc.). Lower intensity surfaces (roads, rooftops, still/calm water) experience higher laser noise. The laser noise range for this survey was approximately 0.02 meters.

Relative Accuracy

Relative accuracy refers to the internal consistency of the data set - the ability to place a laser point in the same location over multiple flight lines, GPS conditions, and aircraft attitudes. Affected by system attitude offsets, scale, and GPS/IMU drift, internal consistency is measured as the divergence between points from different flight lines within an overlapping area. Divergence is most apparent when flight lines are opposing. When the LiDAR system is well calibrated, the line-to-line divergence is low (<10 cm). See Appendix A for further information on sources of error and operational measures that can be taken to improve relative accuracy.

Relative Accuracy Calibration Methodology

1. Manual System Calibration: Calibration procedures for each mission require solving geometric relationships that relate measured swath-to-swath deviations to misalignments of system attitude parameters. Corrected scale, pitch, roll and heading offsets were calculated and applied to resolve misalignments. The raw divergence between lines was computed after the manual calibration was completed and reported for each survey area.
2. Automated Attitude Calibration: All data were tested and calibrated using TerraMatch automated sampling routines. Ground points were classified for each individual flight line and used for line-to-line testing. System misalignment offsets (pitch, roll and

heading) and scale were solved for each individual mission and applied to respective mission datasets. The data from each mission were then blended when imported together to form the entire area of interest.

3. Automated Z Calibration: Ground points per line were used to calculate the vertical divergence between lines caused by vertical GPS drift. Automated Z calibration was the final step employed for relative accuracy calibration.

4.2 Absolute Accuracy

The vertical accuracy of the LiDAR data is described as the mean and standard deviation (sigma ~ σ) of divergence of LiDAR point coordinates from RTK ground survey point coordinates. To provide a sense of the model predictive power of the dataset, the root mean square error (RMSE) for vertical accuracy is also provided. These statistics assume the error distributions for x, y, and z are normally distributed, thus we also consider the skew and kurtosis of distributions when evaluating error statistics.

Statements of statistical accuracy apply to fixed terrestrial surfaces only and may not be applied to areas of dense vegetation or steep terrain (See Appendix A). To calibrate laser accuracy for the Delivery 11 LiDAR dataset 6451 RTK points were collected in UTM 11 on fixed, hard-packed road surfaces within the survey area.

5. Study Area Results

Summary statistics for point resolution and accuracy (relative and absolute) of the LiDAR data collected in the Columbia River survey areas are presented below in terms of central tendency, variation around the mean, and the spatial distribution of the data (for point resolution by quadrangle).

5.1 Data Summary

Table 3. Resolution and Accuracy - Specifications and Achieved Values

	Targeted	Achieved
†**Resolution:**		
UTM 11	≥ 8 points/m^2	6.01 points/m^2
***Vertical Accuracy (1 σ):**		
UTM 11	<13 cm	4.7 cm

† The final delivered density will exclude large water features resulting in a more accurate ground and native density.
* Based on 28,317 hard-surface control points collected within UTM 11.

5.2 Data Density/Resolution

The average first-return density of the UTM 11 delivered dataset is 6.01 points per square meter (**Table 3**). The initial dataset, acquired to be 8 points per square meter, was filtered as described previously to remove spurious or inaccurate points. Additionally, some types of surfaces (i.e., dense vegetation, breaks in terrain, steep slopes, water) may return fewer pulses (delivered density) than the laser originally emitted (native density). Due to the fact that this survey focused on a narrow corridor buffering the Columbia River and other large water bodies, the reported first return density is artificially low.
Ground classifications were derived from automated ground surface modeling and manual, supervised classifications where it was determined that the automated model had failed. Ground return densities will be lower in areas of dense vegetation, water, or buildings.
The maps in **Figures 5 - 31** identify the average native and ground point densities for each USGS 0.75 minute quad. Tiles with greater than 20 million points were divided in half to keep LAS file sizes manageable.

Cumulative LiDAR data resolution for UTM 11 of the Columbia River survey:

- Average Point (First Return) Density = 6.01 points/m^2
- Average Ground Point Density = 1.55 points/m^2

Figure 3. Density distribution for first return laser points in UTM 11.

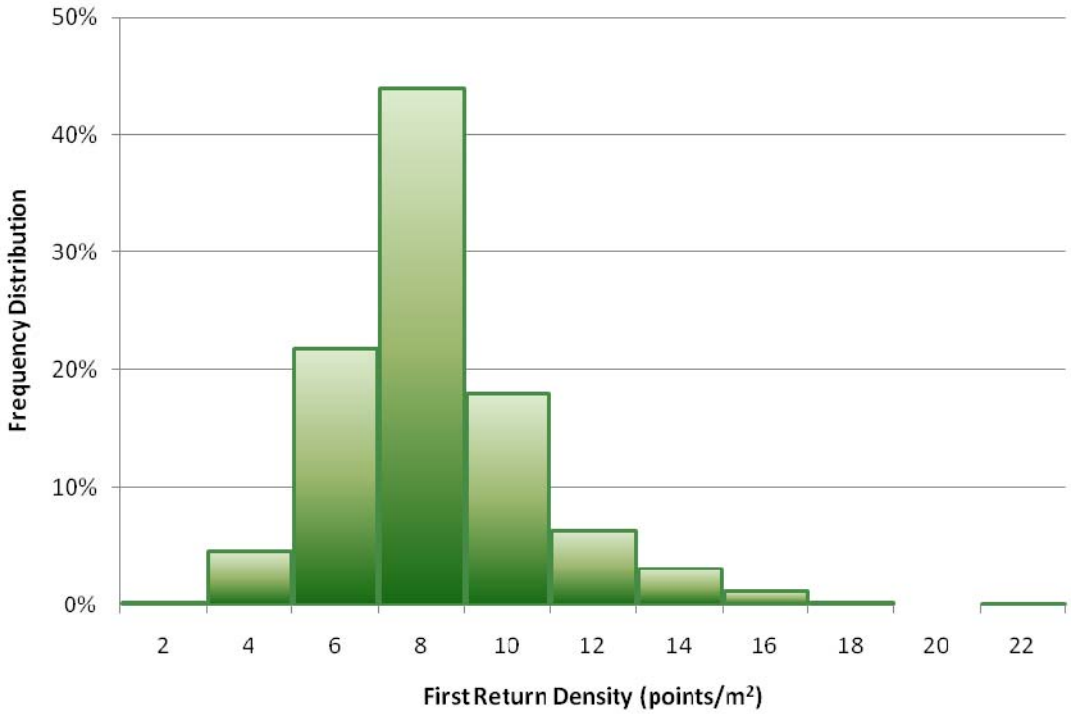

Figure 4. Density distribution for ground-classified laser points in, UTM 11.

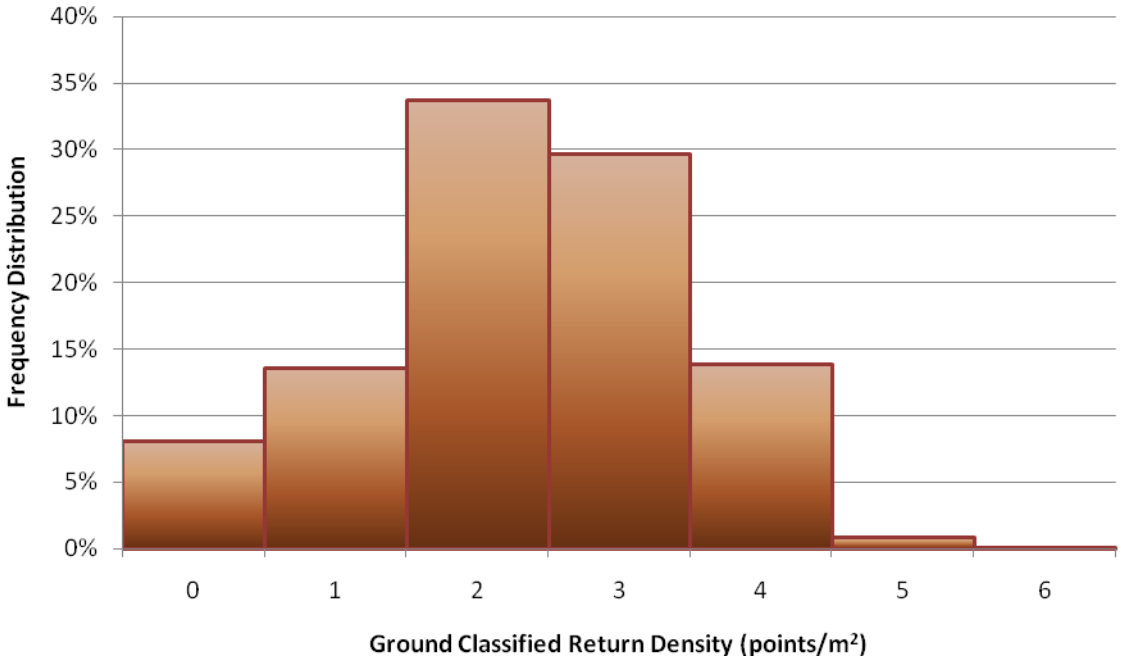

Figure 5. Delivery 1, UTM 10 density distribution map for first return points by USGS 0.75 minute quads.

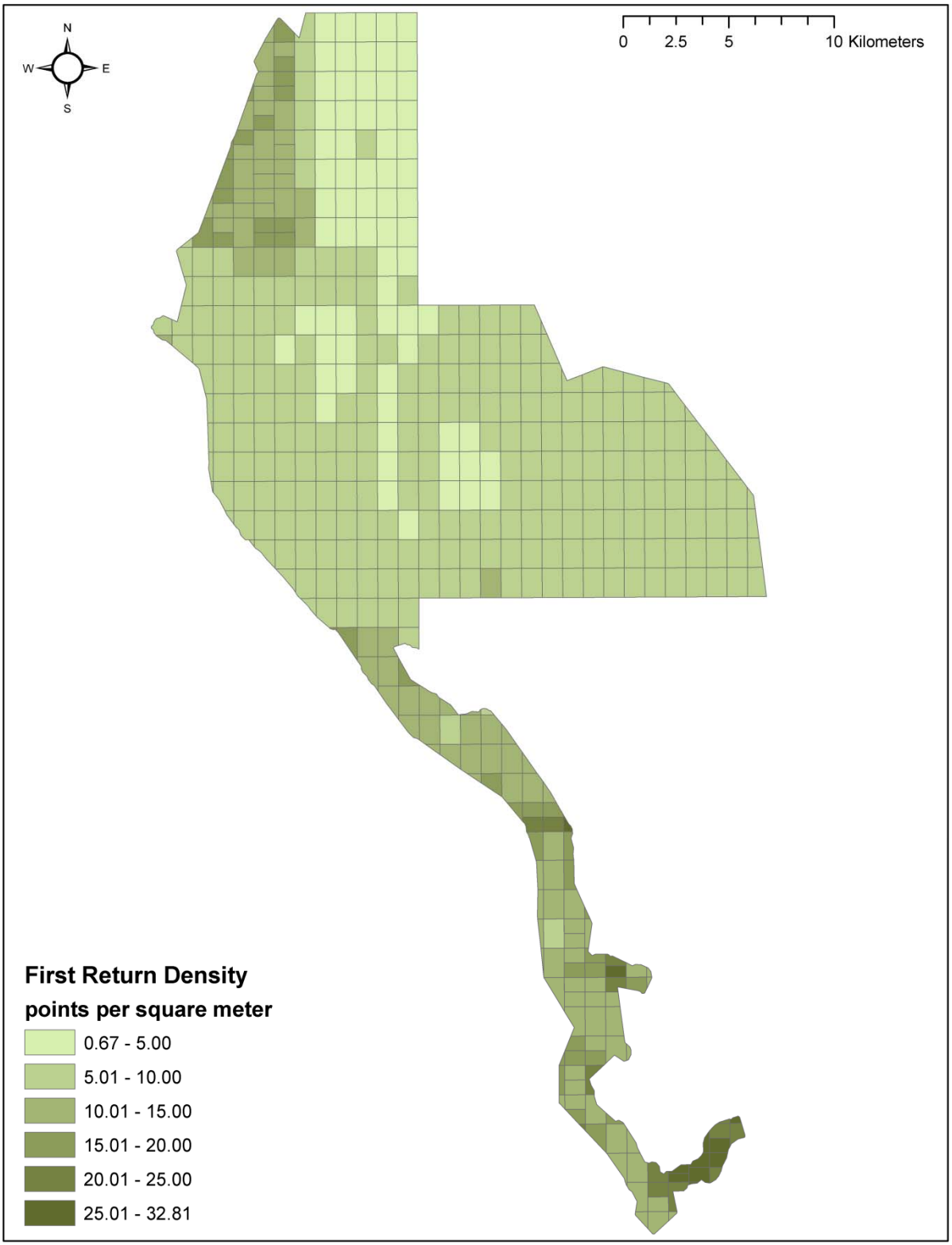

Figure 6. Delivery 1, UTM 10 density distribution map for ground return points by USGS 0.75 minute quads.

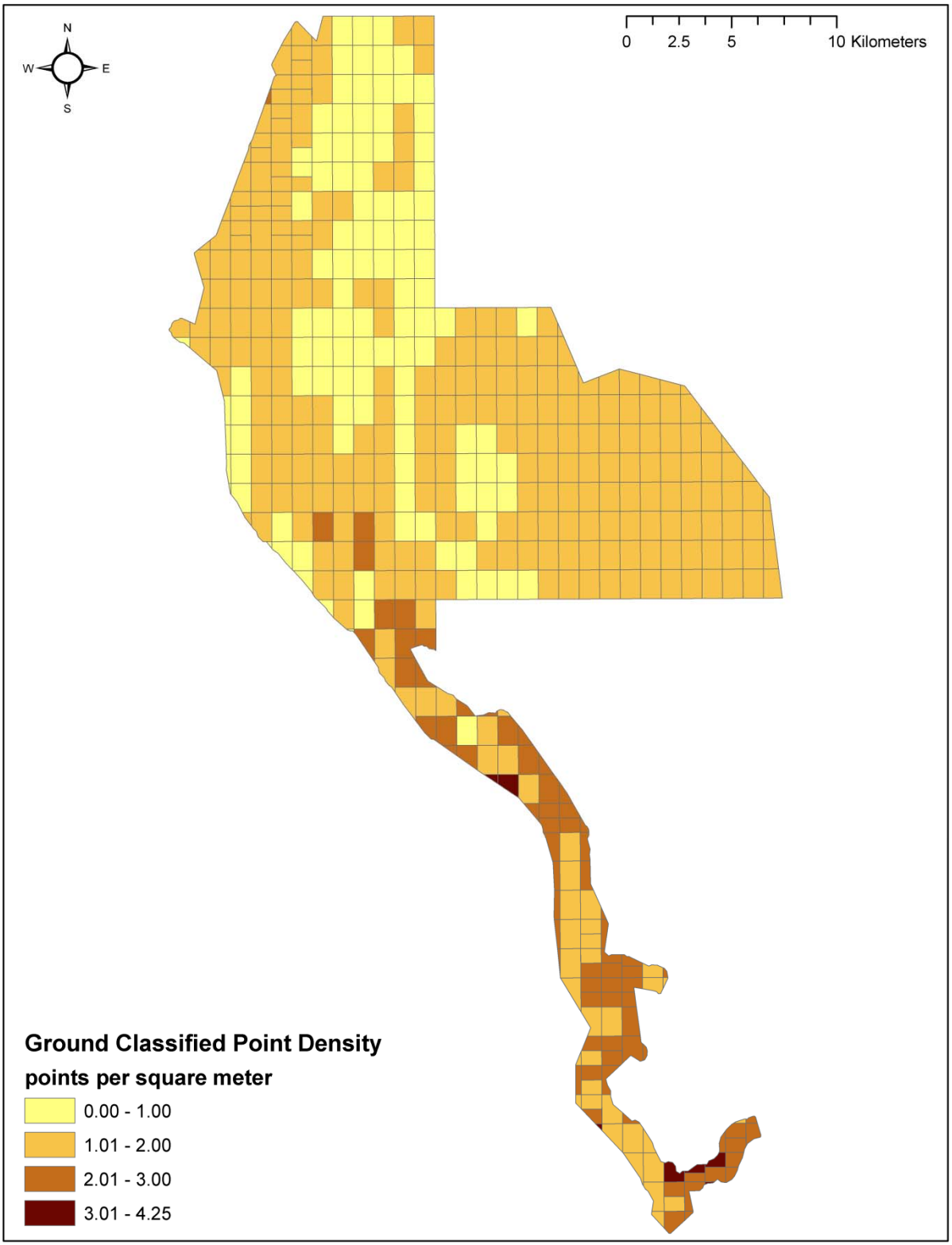

Figure 7. Delivery 1, UTM 11 density distribution map for first return points by USGS 0.75 minute quads.

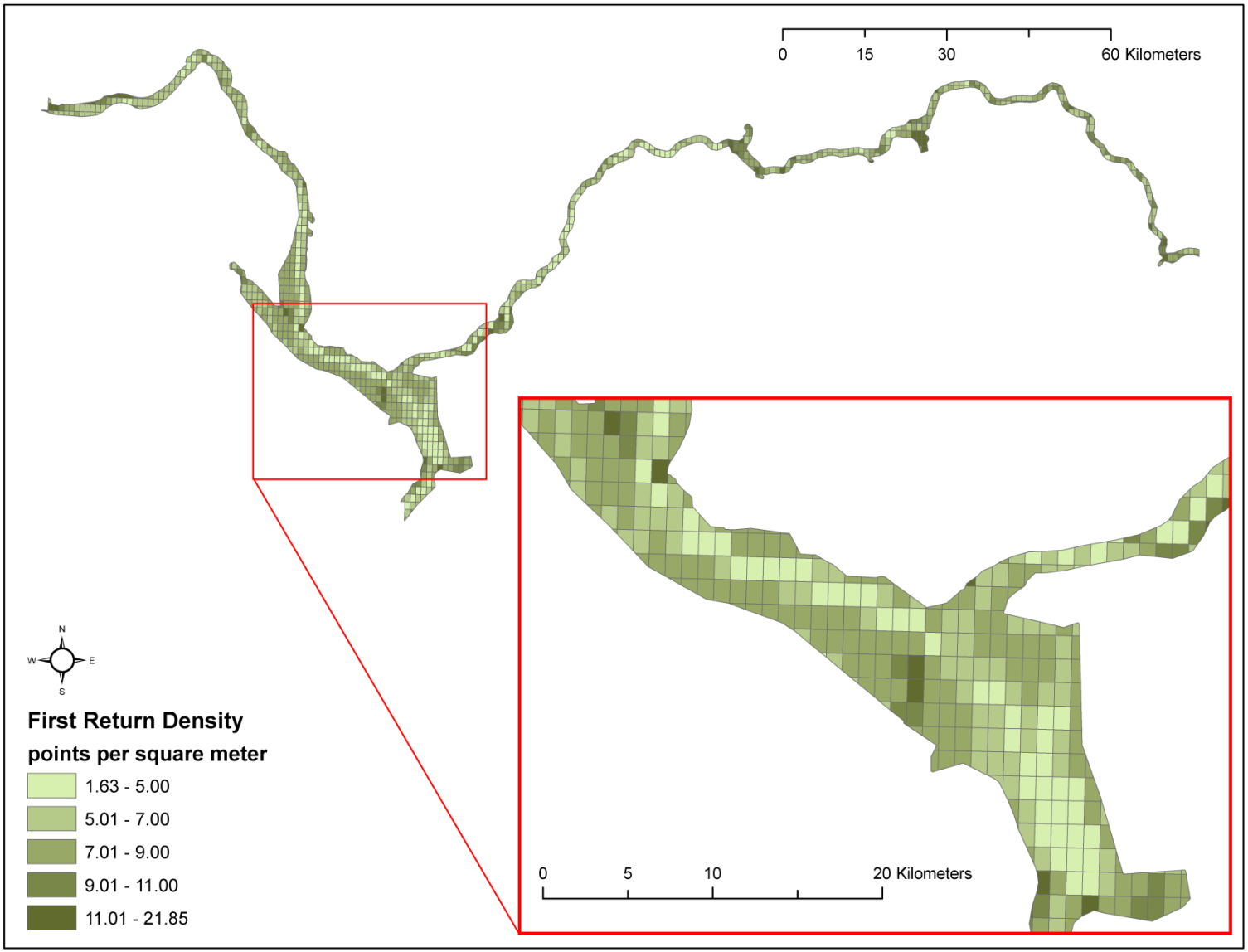

Figure 8. Delivery 1, UTM 11 density distribution map for ground return points by USGS 0.75 minute quads.

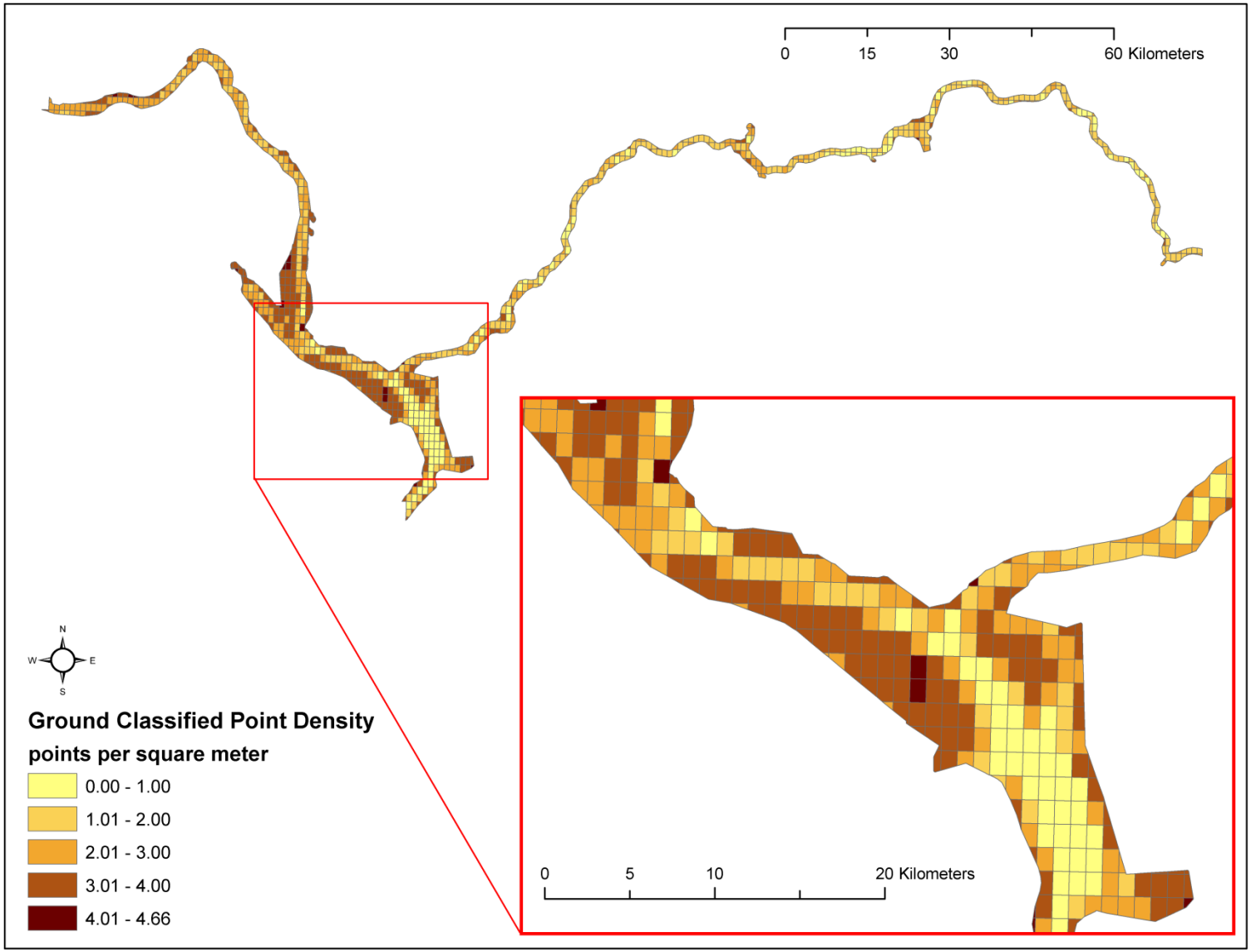

Figure 9. Delivery 2, UTM 10 density distribution map for first return points by USGS 0.75 minute quads.

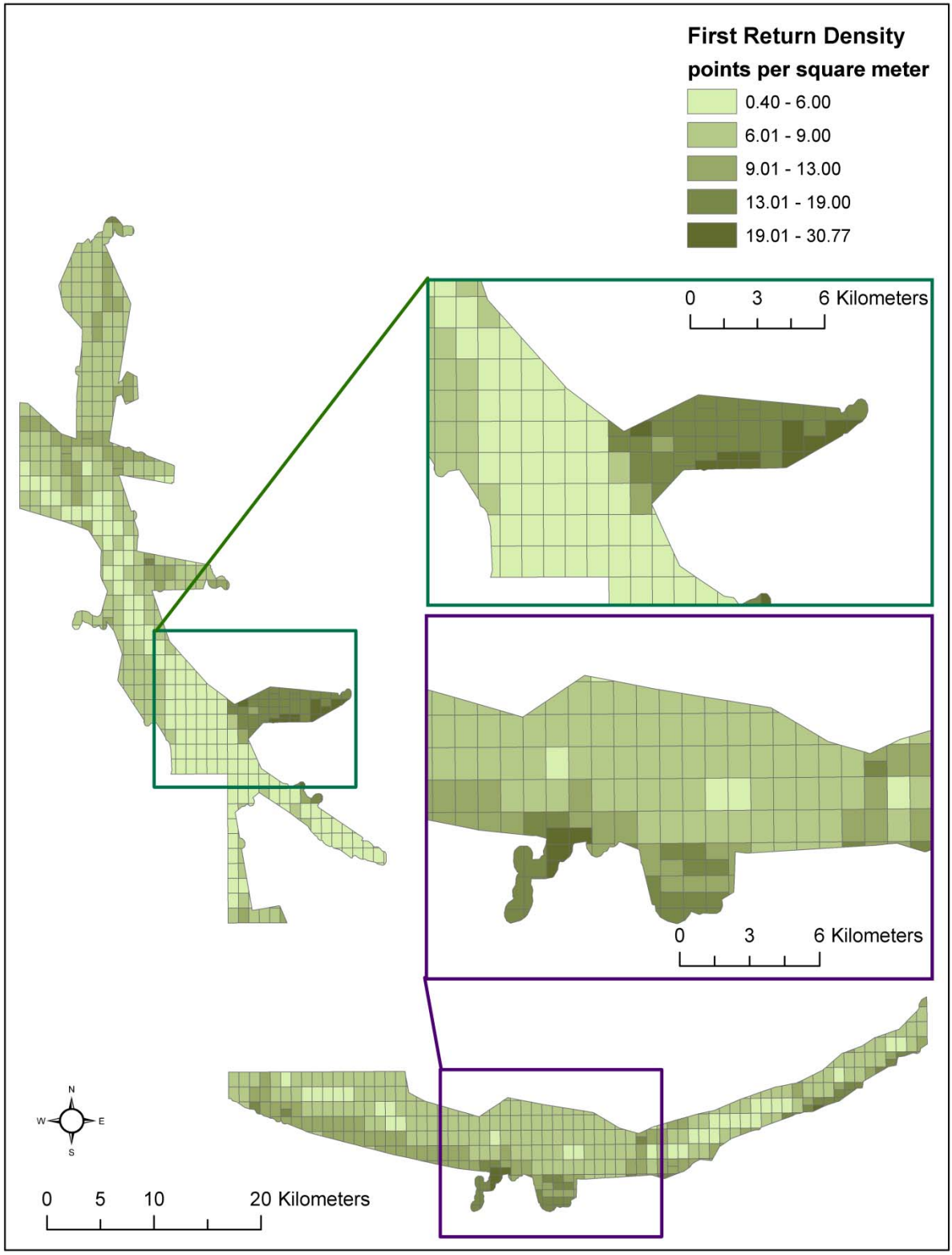

Figure 10. Delivery 2, UTM 10 density distribution map for ground return points by USGS 0.75 minute quads.

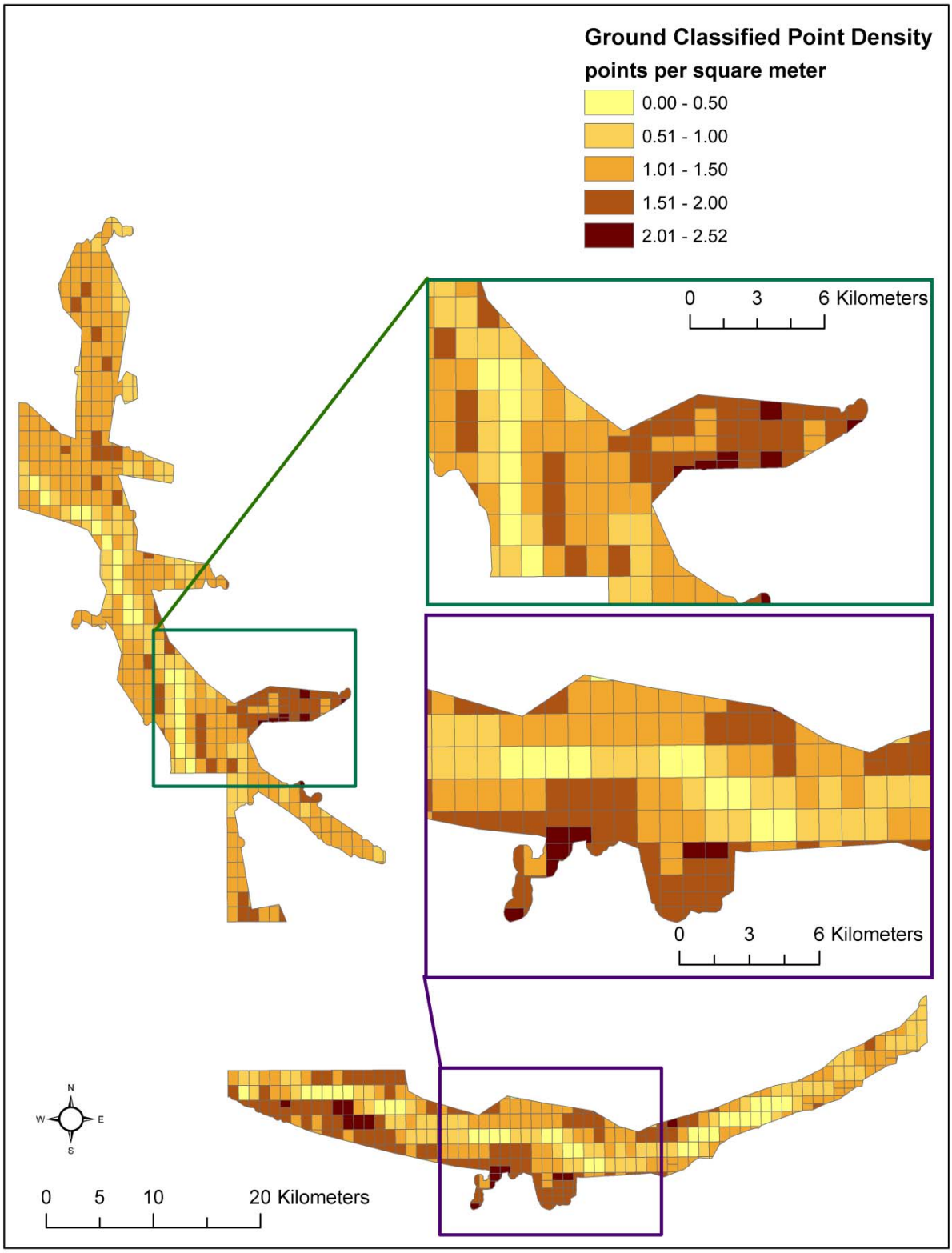

Figure 11. Delivery 3, UTM 11 density distribution map for first return points by USGS 0.75 minute quads

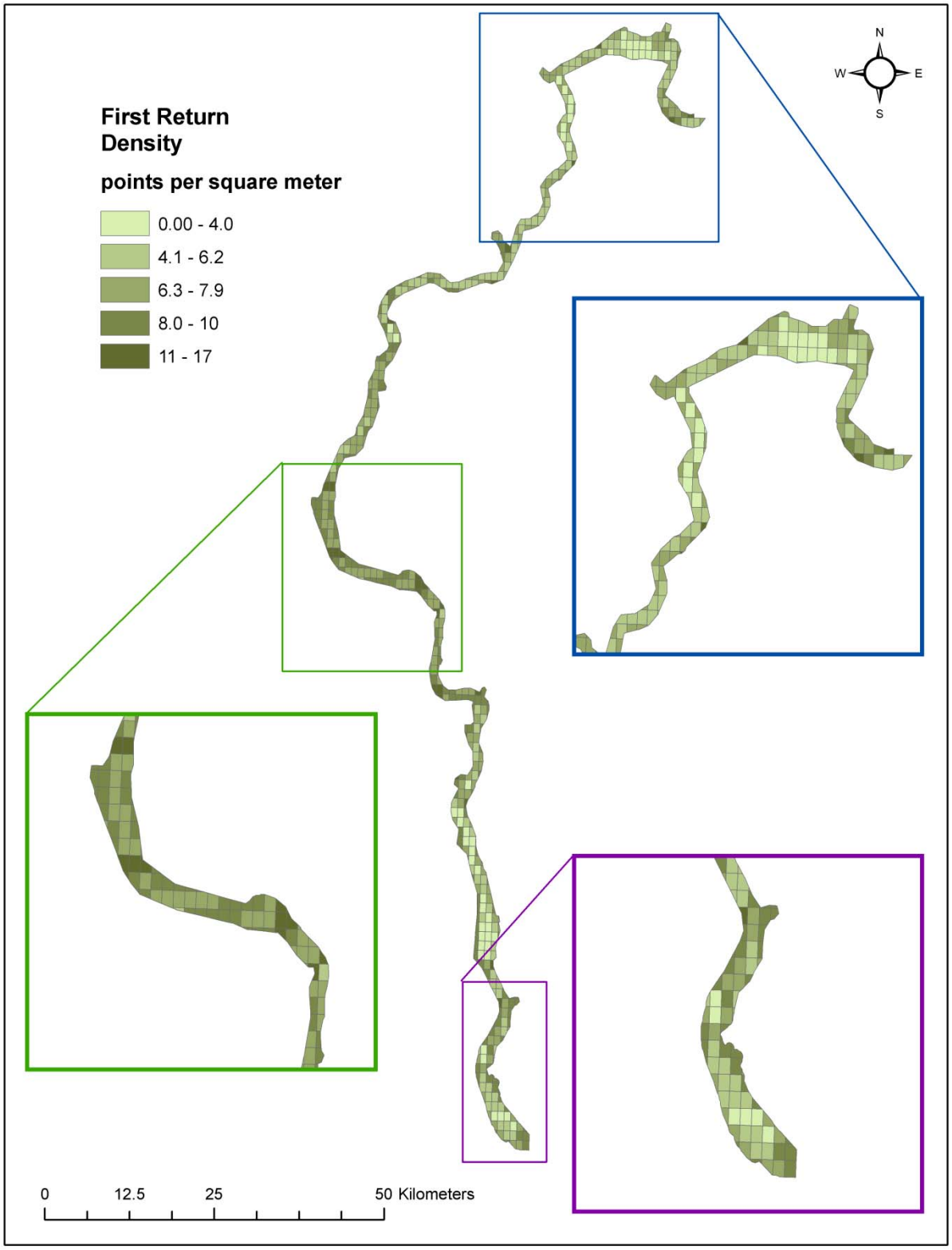

Figure 12. Delivery 3, UTM 11 density distribution map for ground return points by USGS 0.75 minute quads.

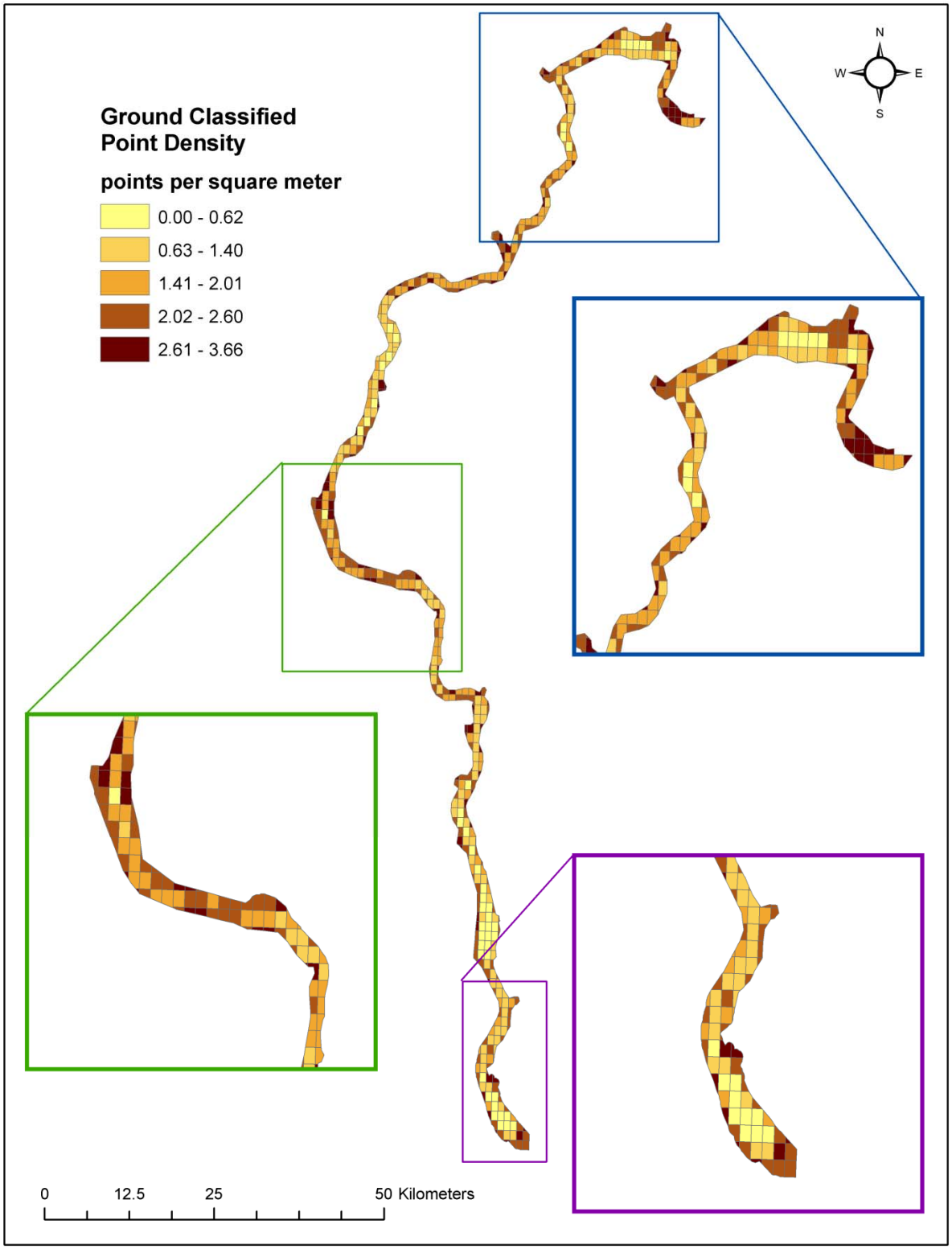

Figure 13. Delivery 4, UTM 10 density distribution map for first return points by USGS 0.75 minute quads.

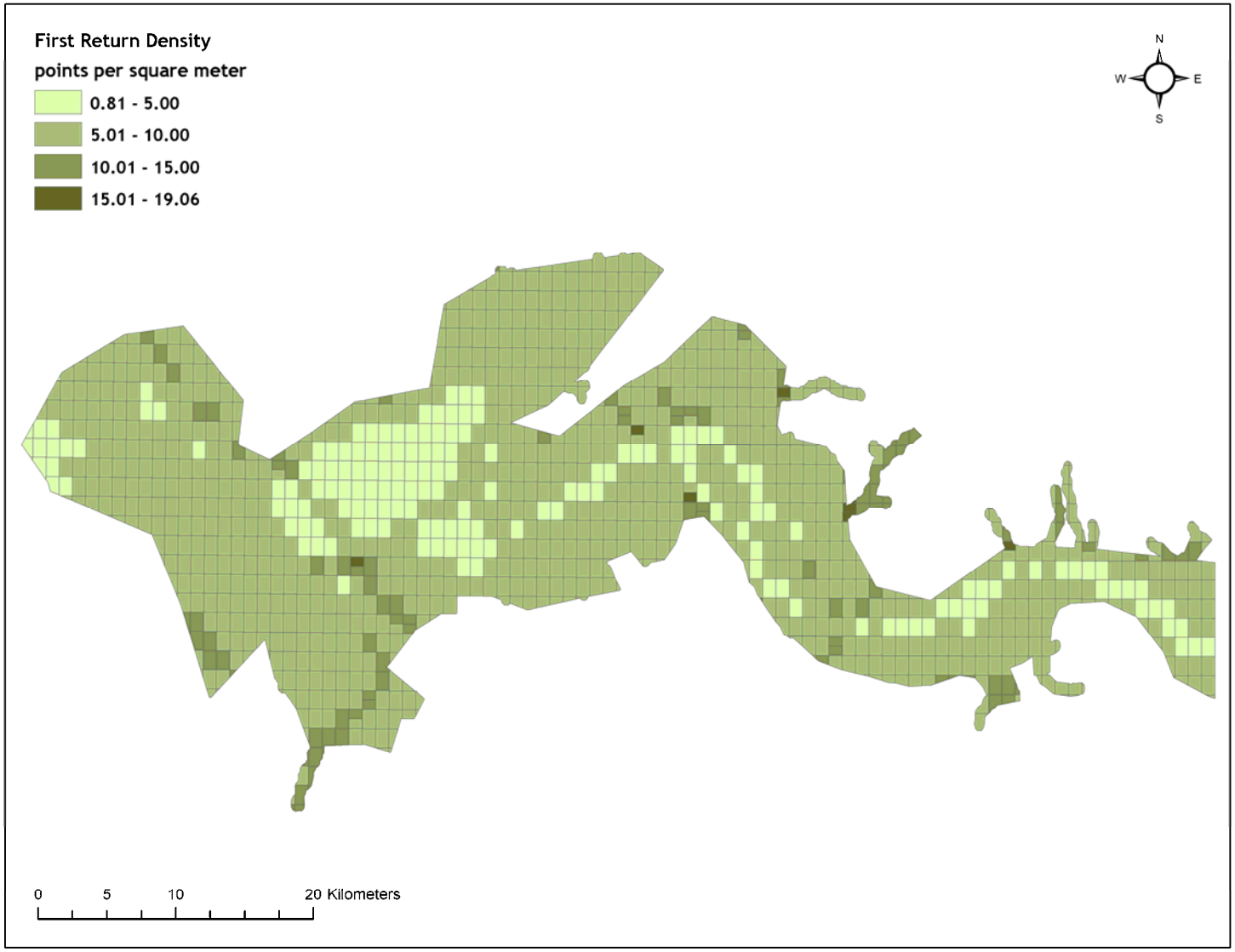

Figure 14. Delivery 4, UTM 10 density distribution map for ground return points by USGS 0.75 minute quads.

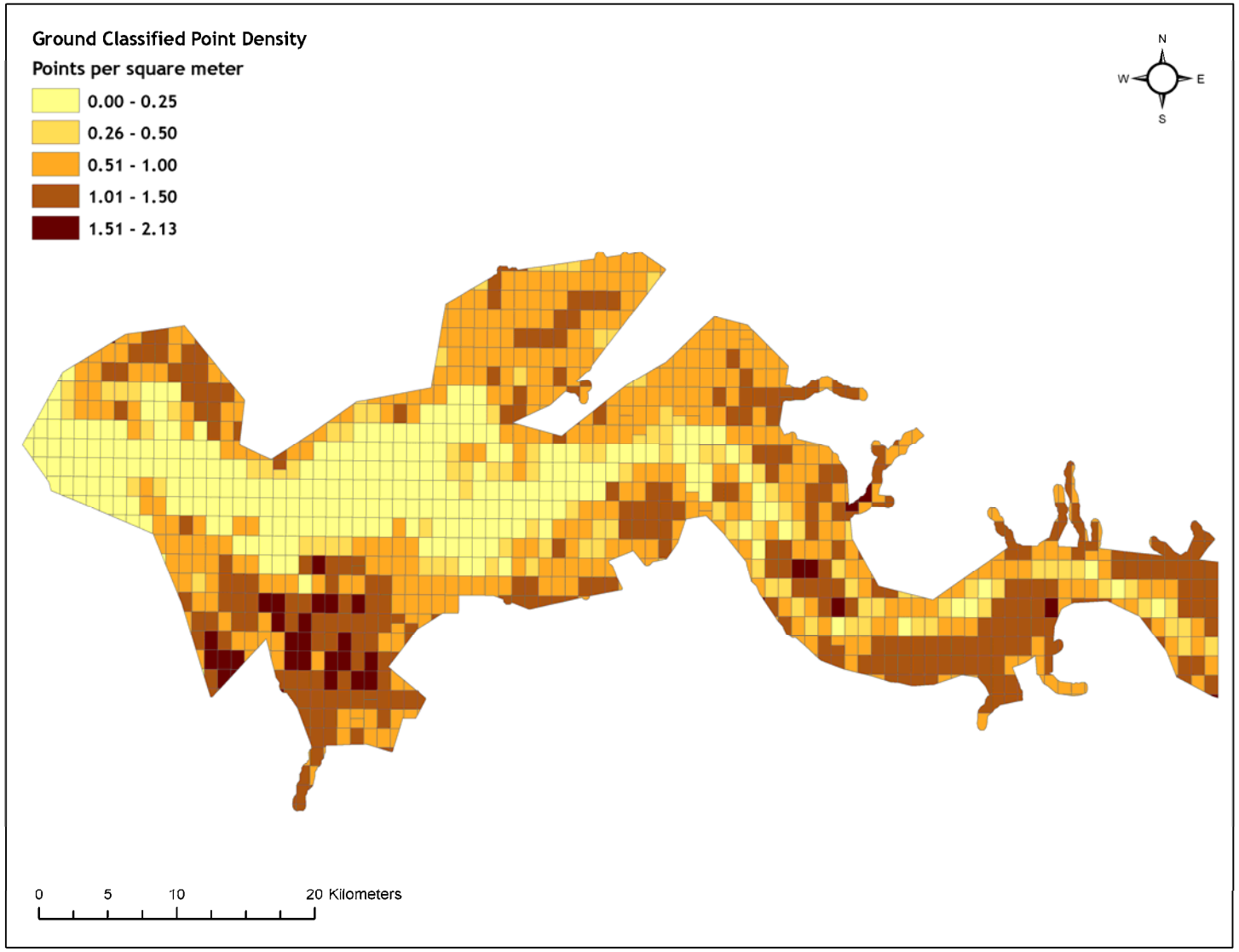

Figure 15. Delivery 5, UTM 11 density distribution map for first return points by USGS 0.75 minute quads.

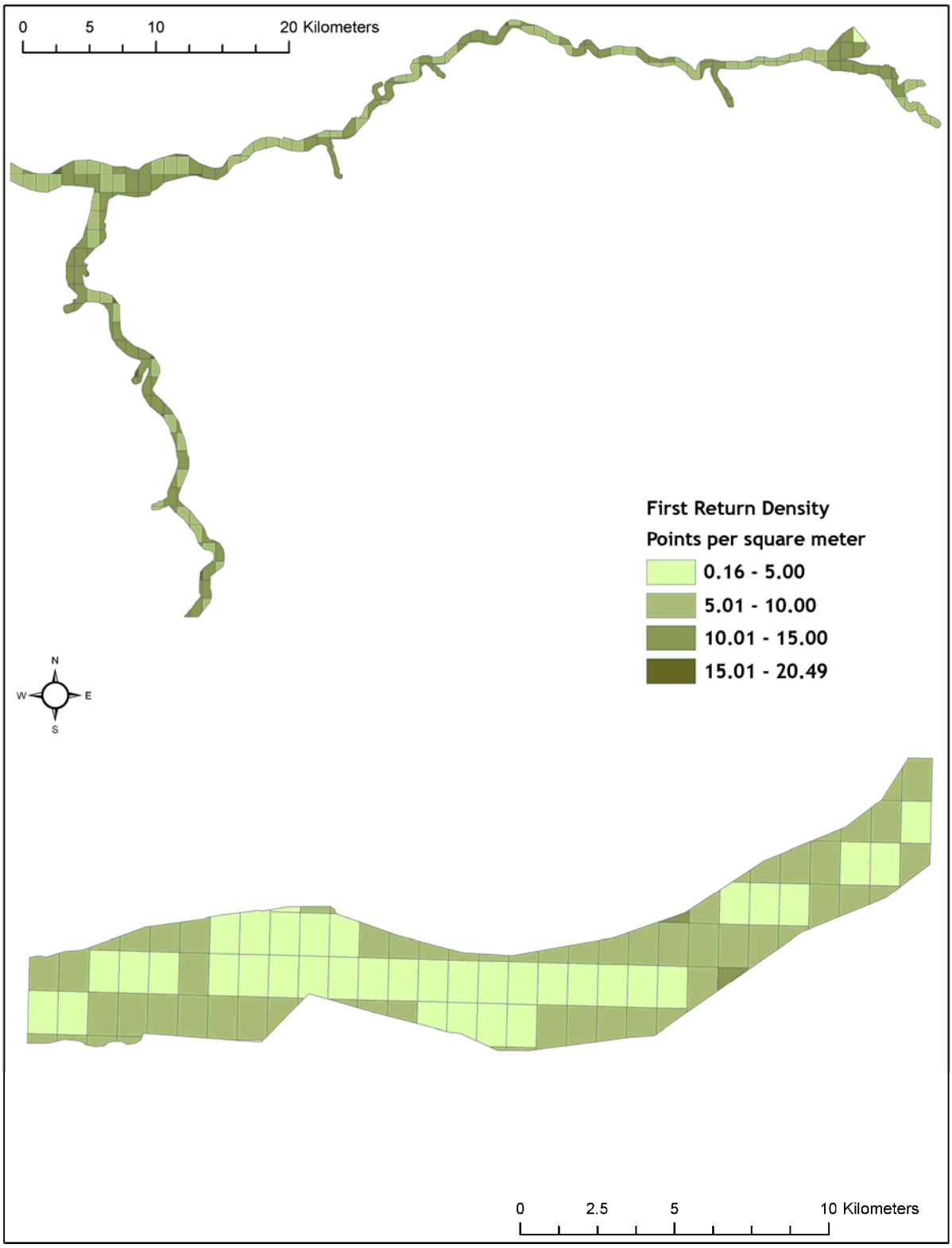

Figure 16. Delivery 5, UTM 11 density distribution map for ground classified points by USGS 0.75 minute quads.

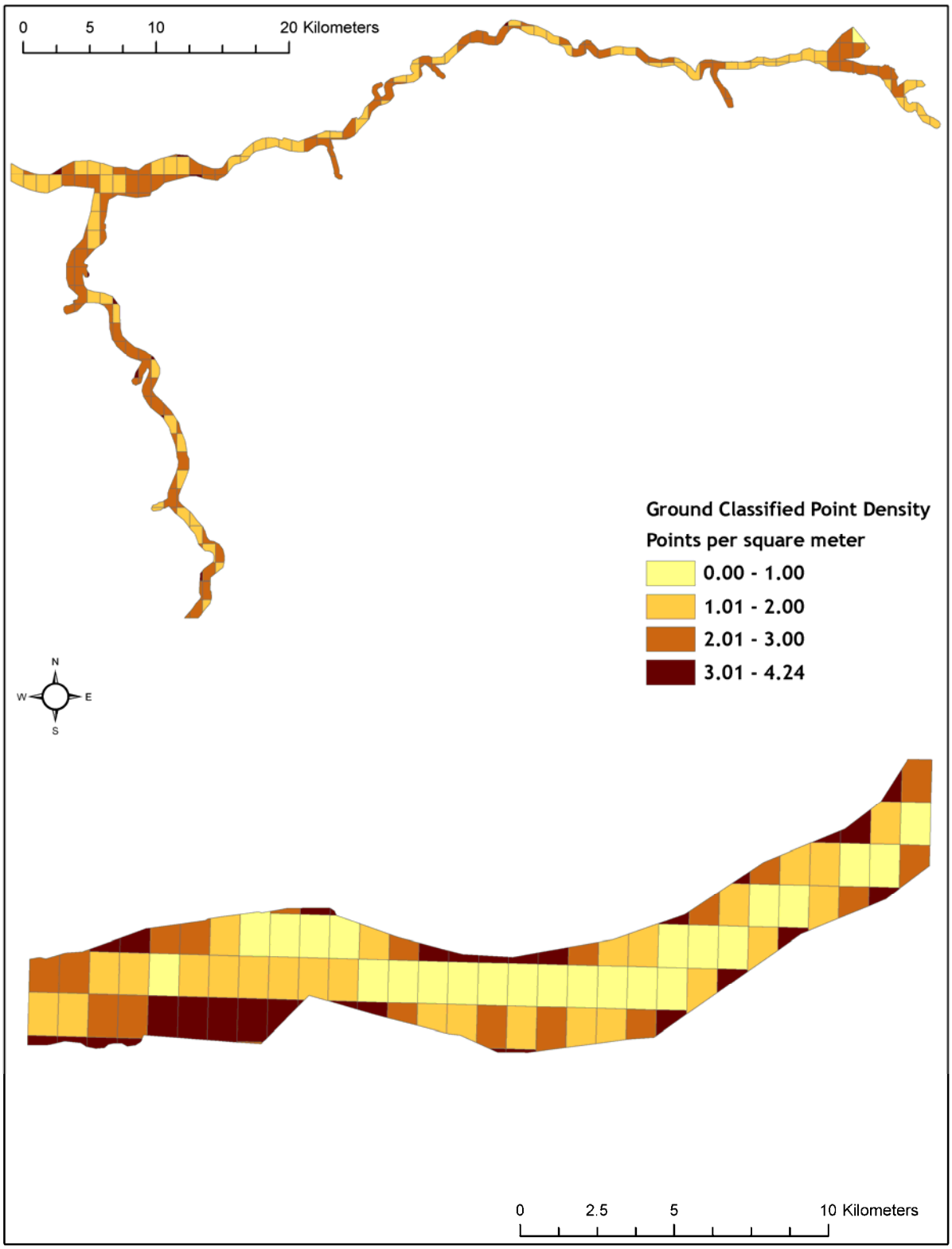

Figure 17. Delivery 6, UTM 11 density distribution map for first return points by USGS 0.75 minute quads.

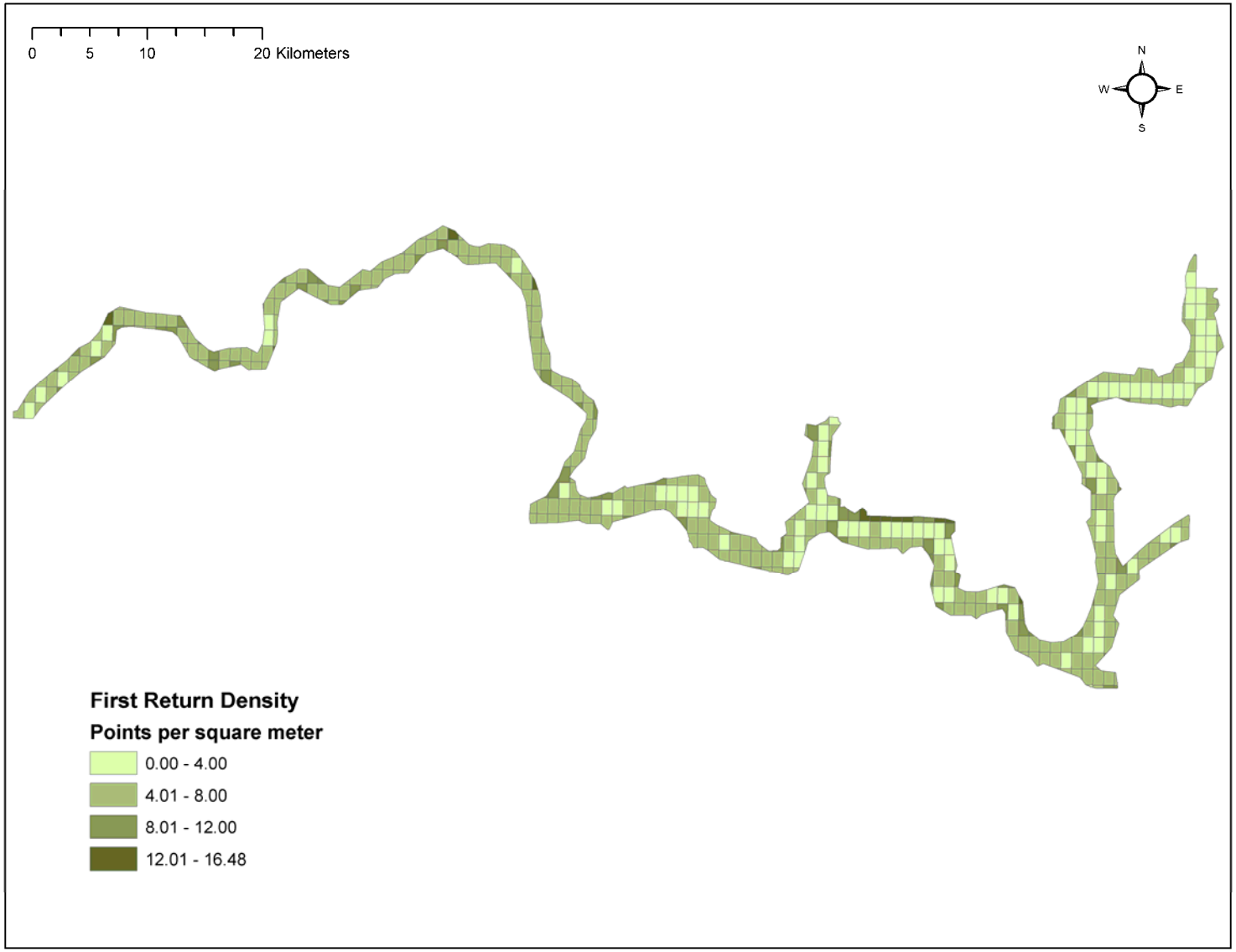

Figure 18. Delivery 6, UTM 11 density distribution map for ground classified points by USGS 0.75 minute quads.

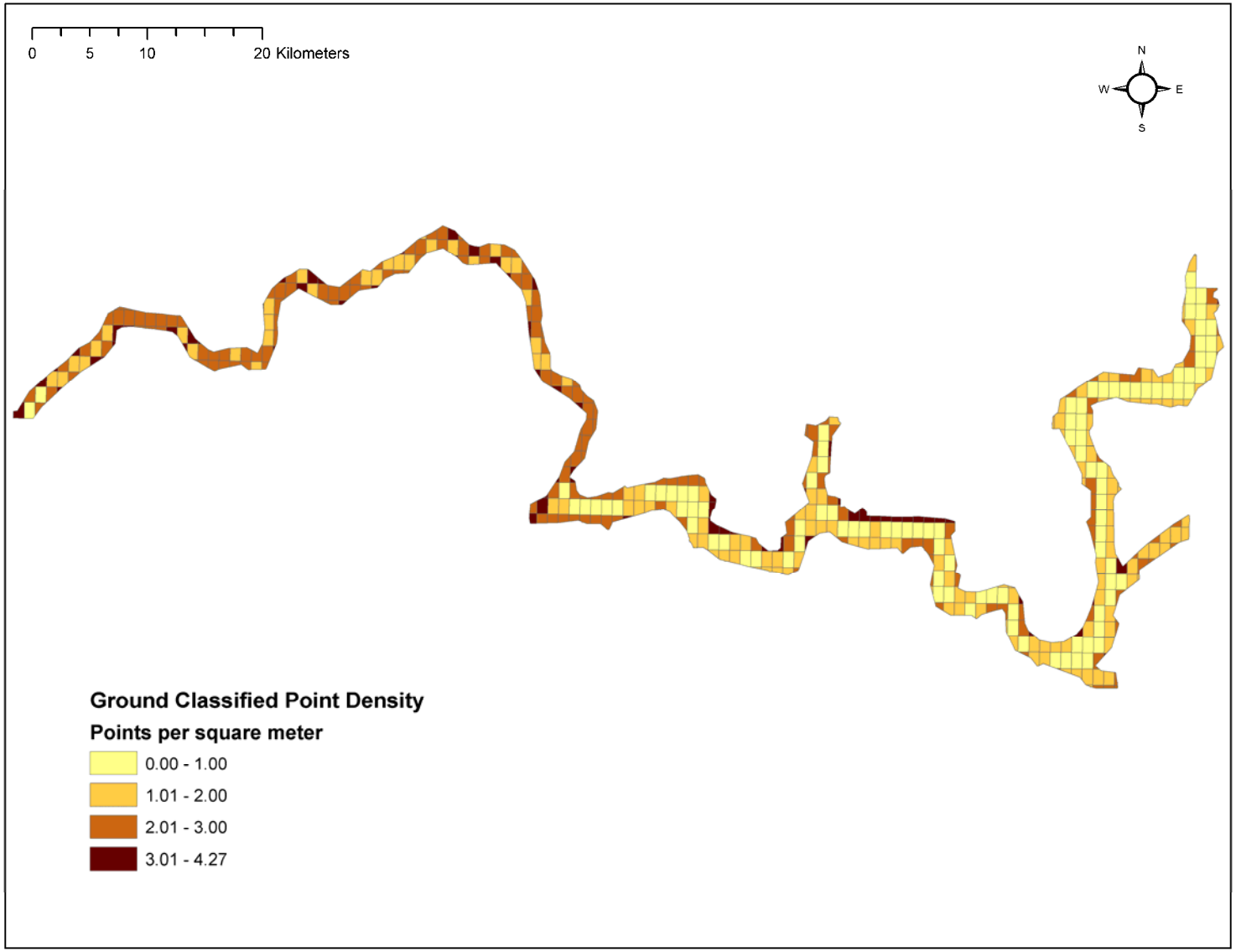

Figure 19. Delivery 6b, UTM 11 density distribution map for first return points by USGS 0.75 minute quads.

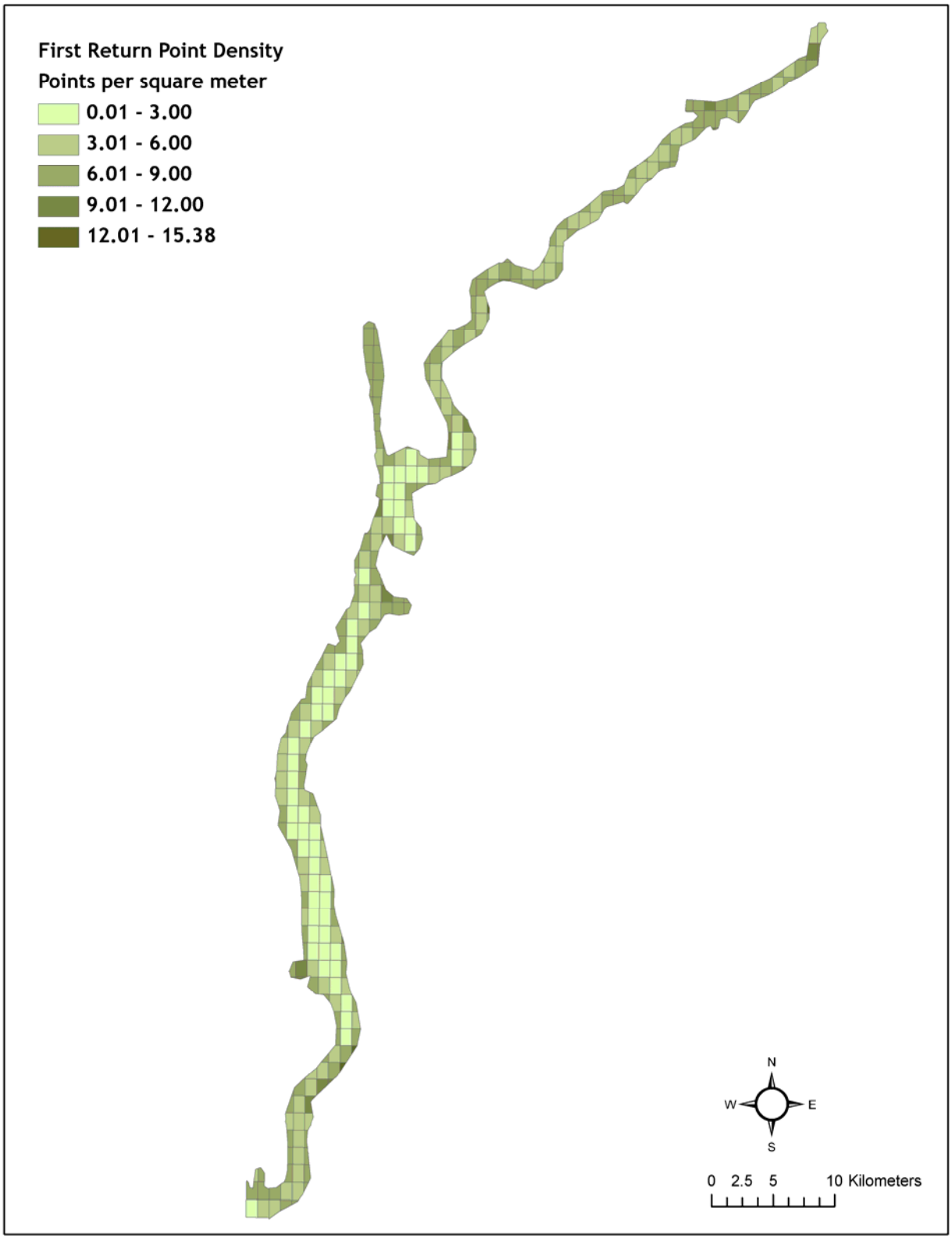

Figure 20. Delivery 6b, UTM 11 density distribution map for ground classified points by USGS 0.75 minute quads.

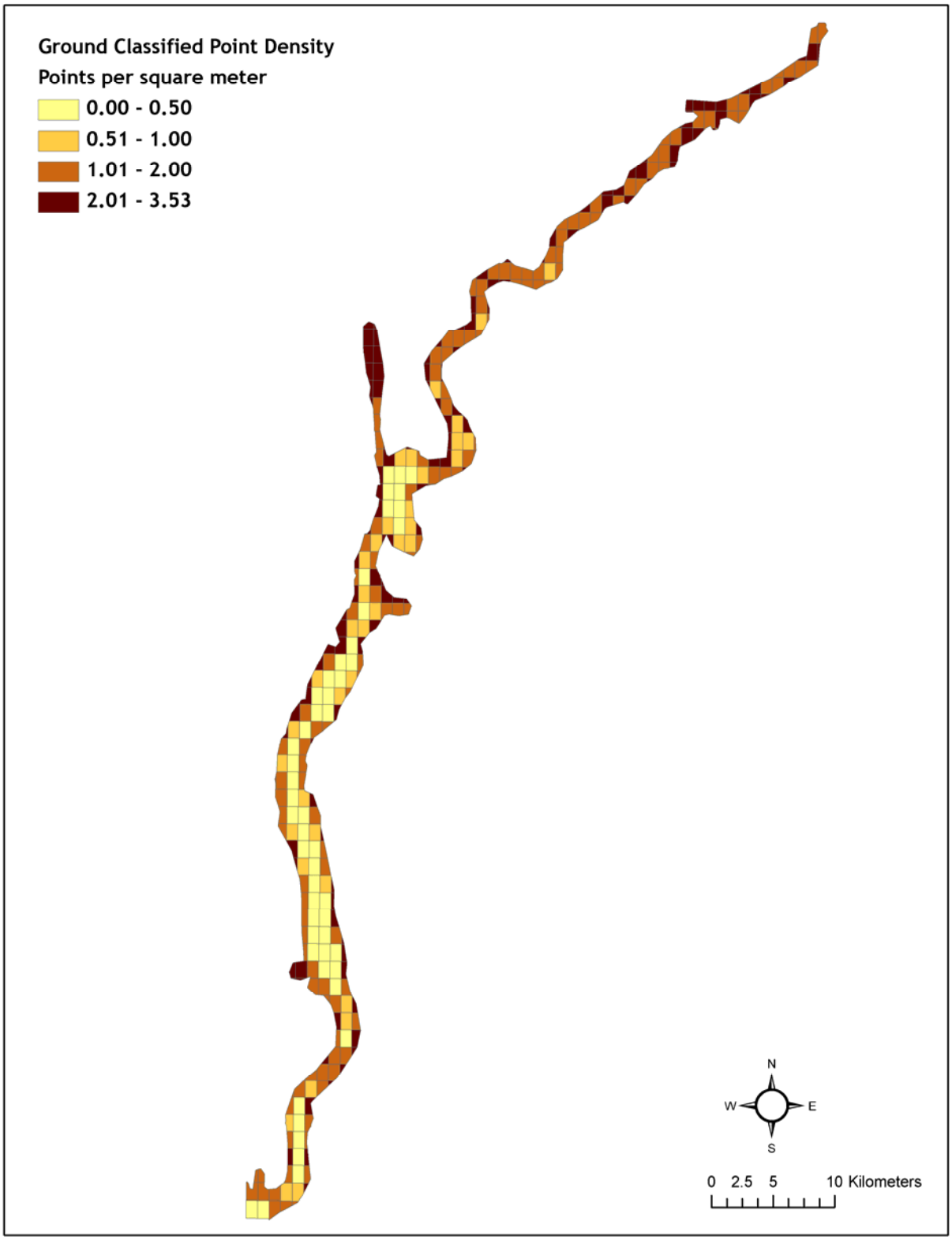

Figure 21. Delivery 7, UTM 11 density distribution map for first return points by USGS 0.75 minute quads.

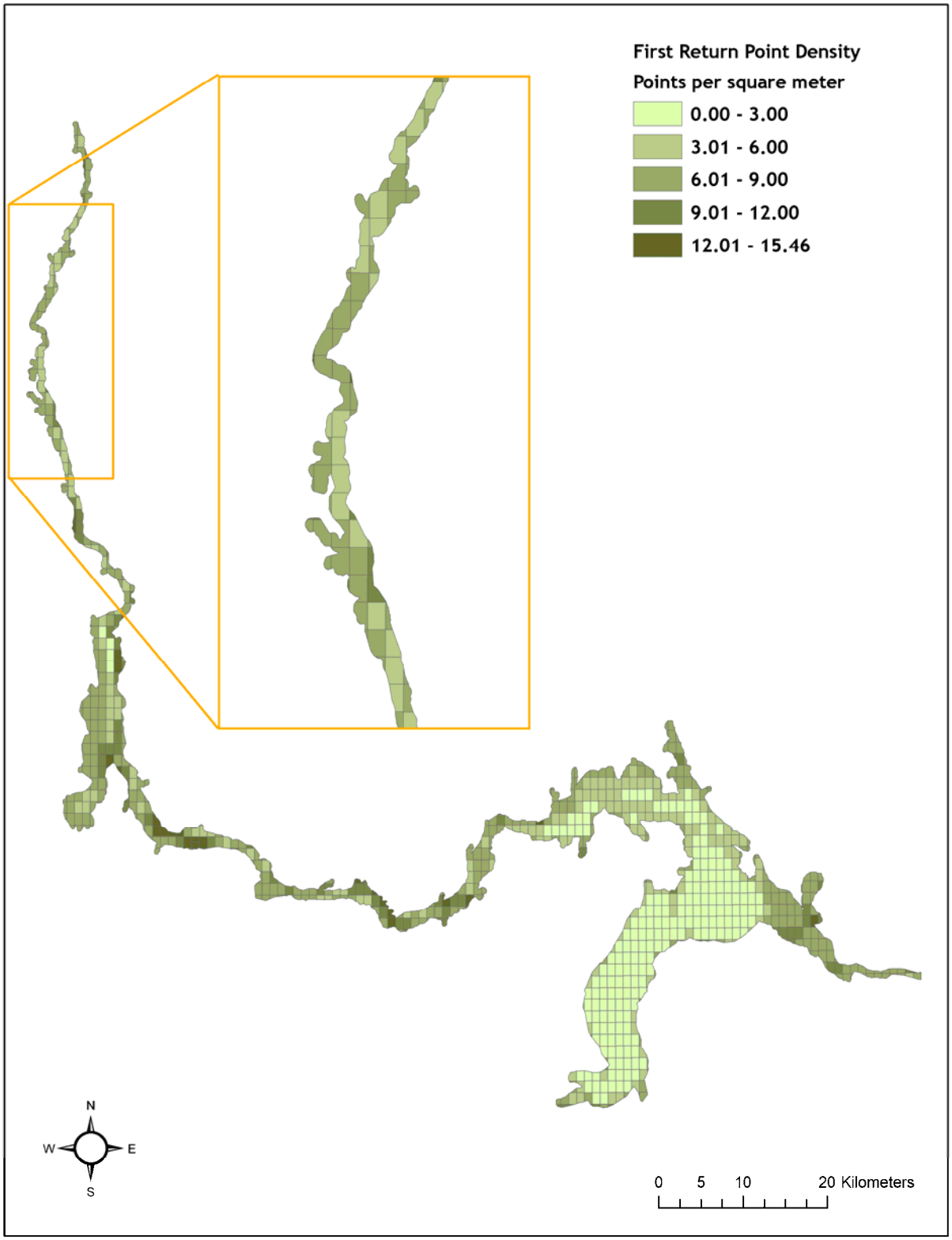

Figure 22. Delivery 7, UTM 11 density distribution map for ground classified points by USGS 0.75 minute quads.

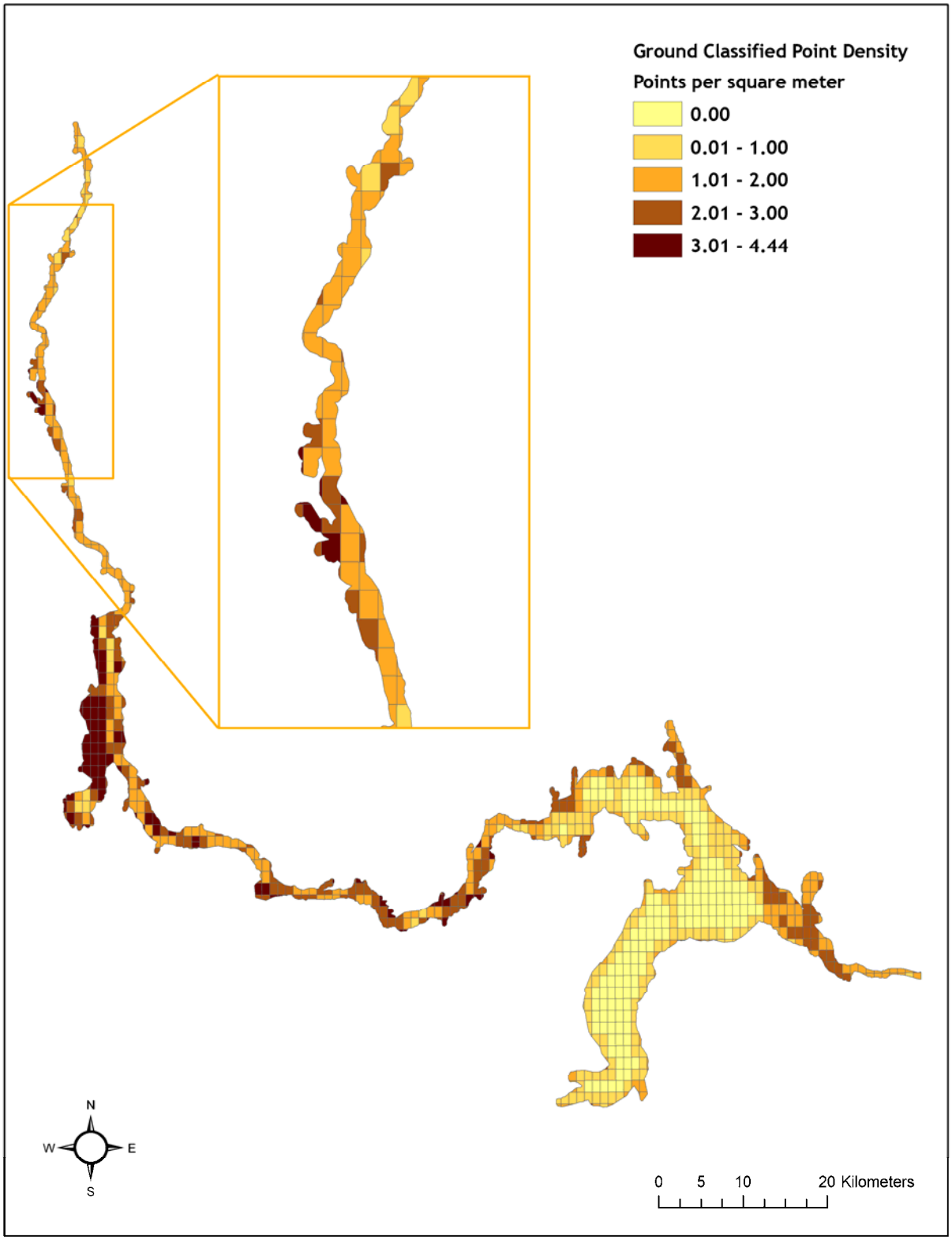

Figure 23. Delivery 8, UTM 10 density distribution map for ground classified and first return points by USGS 0.75 minute quads.

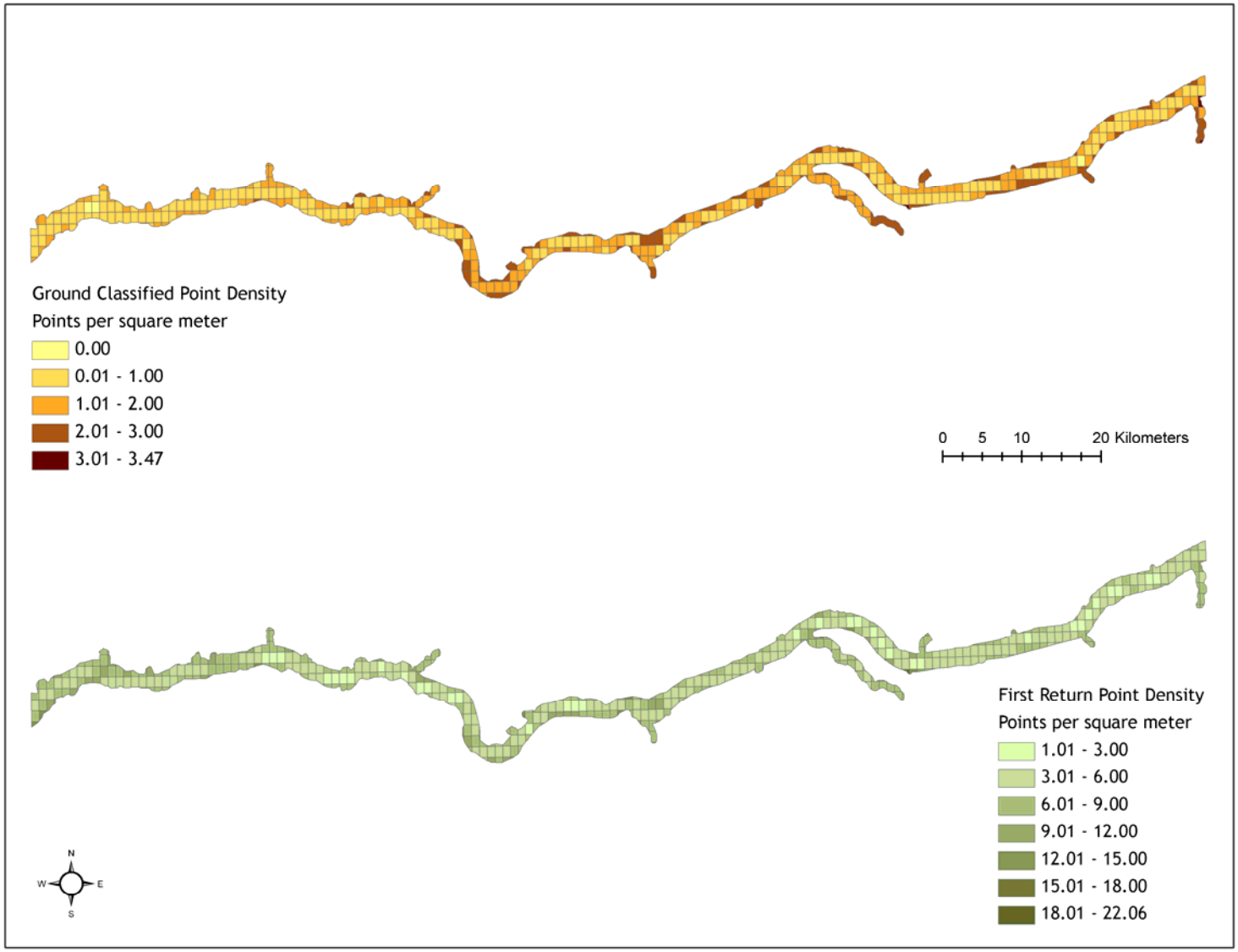

Figure 24. Delivery 8, UTM 11 density distribution map for ground classified and first return points by USGS 0.75 minute quads.

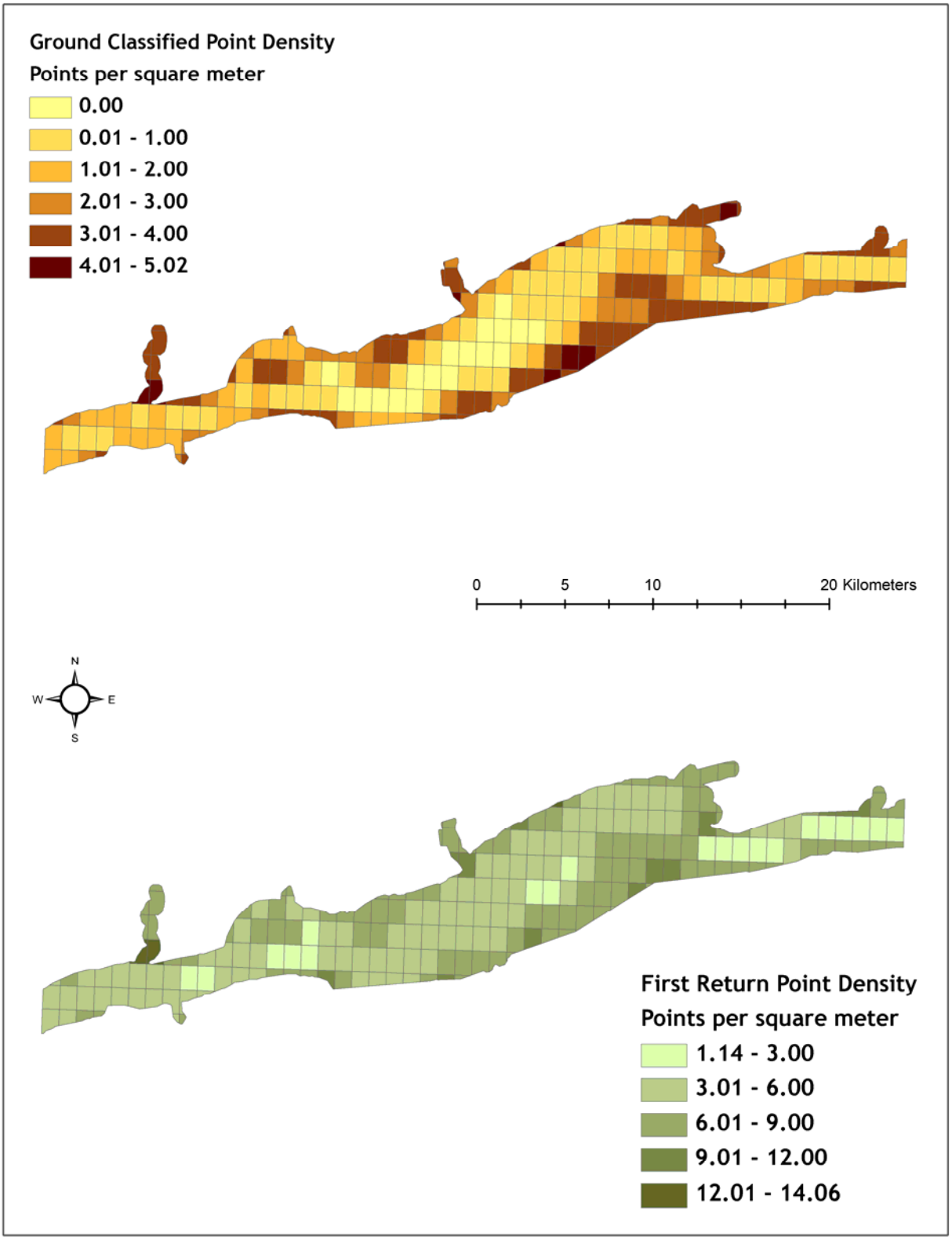

Figure 25. Delivery 9, UTM 11 density distribution map for first return points by USGS 0.75 minute quads.

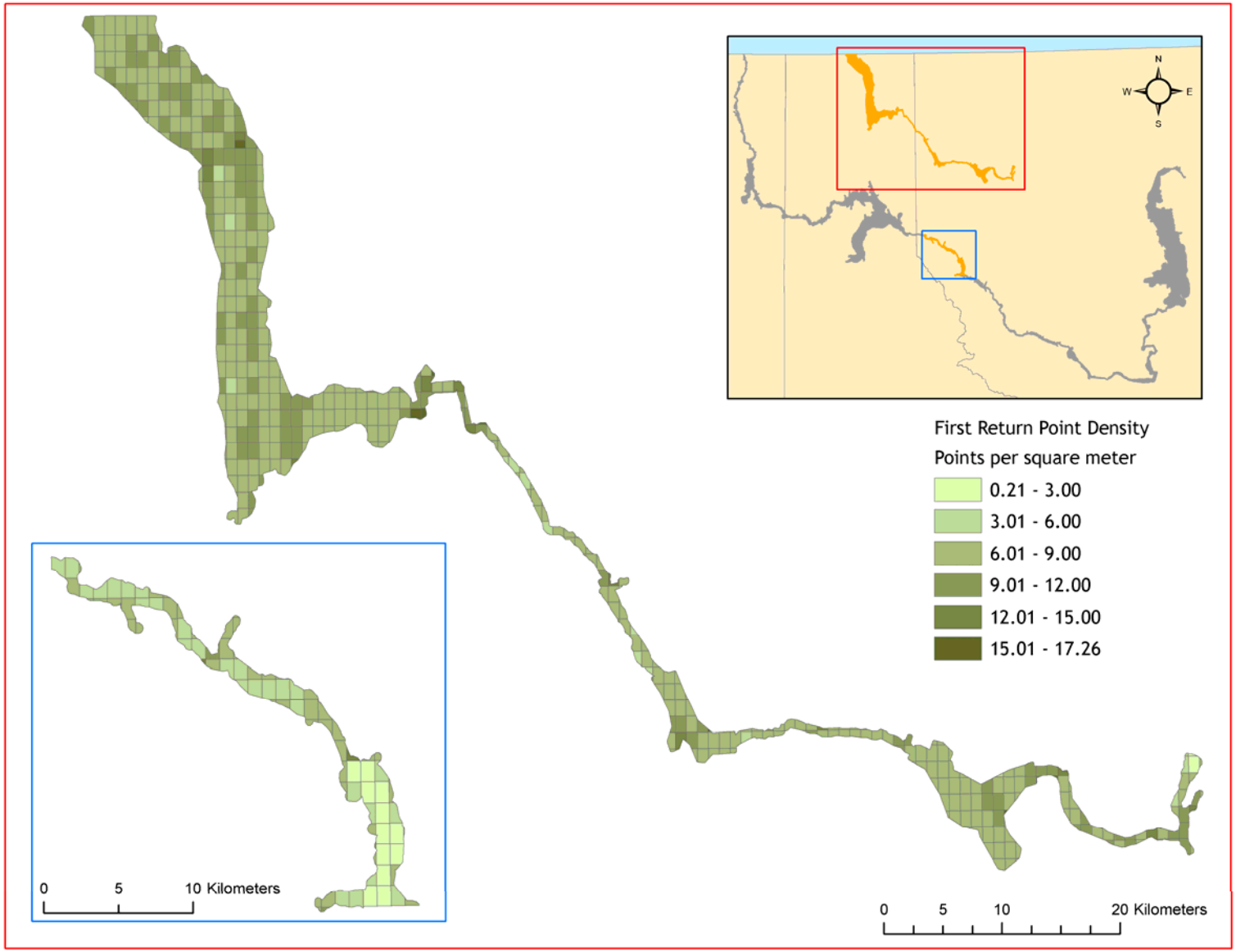

Figure 26. Delivery 9, UTM 11 density distribution map for ground classified points by USGS 0.75 minute quads.

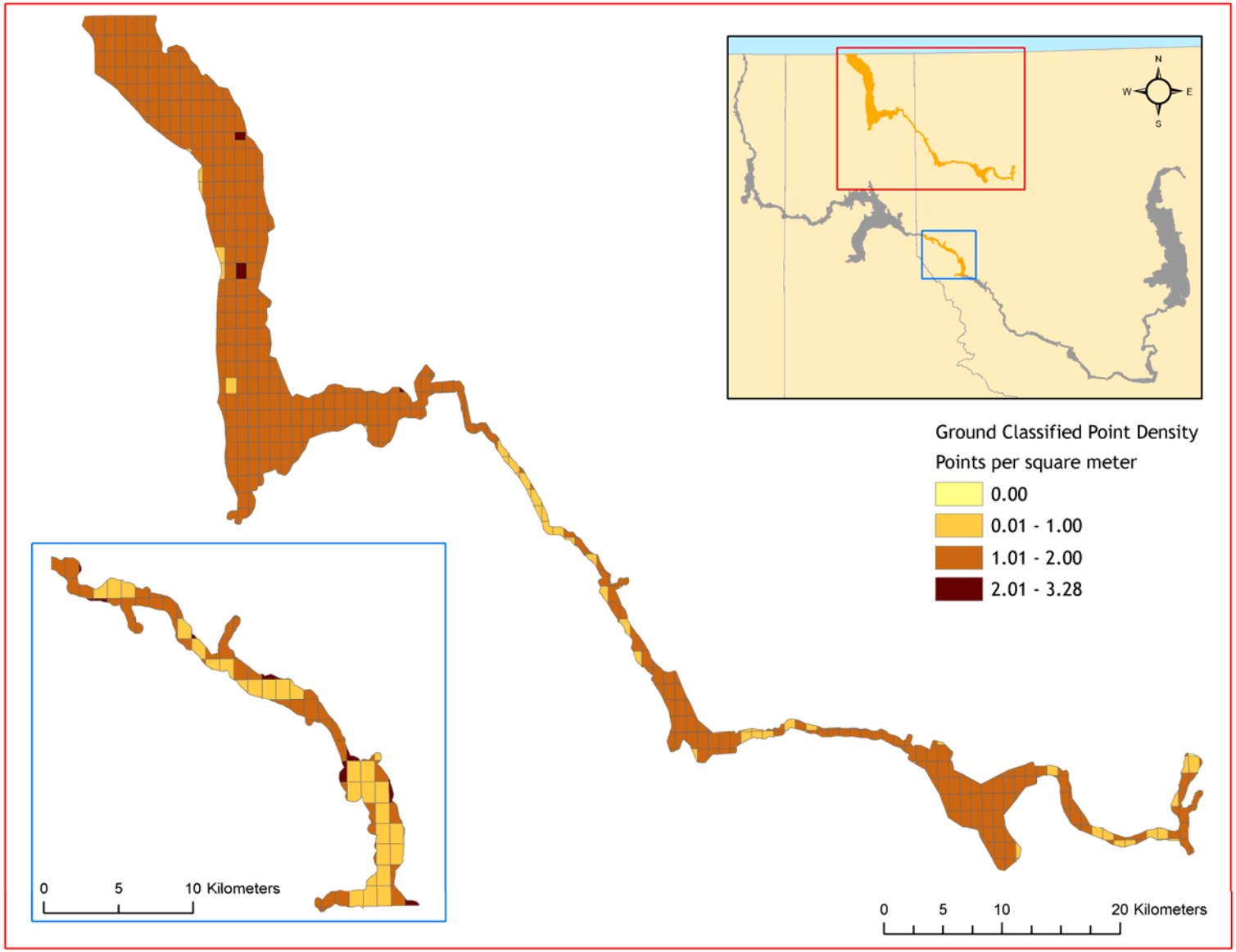

Figure 27. Delivery 10, UTM 11 density distribution map for first return points by USGS 0.75 minute quads.

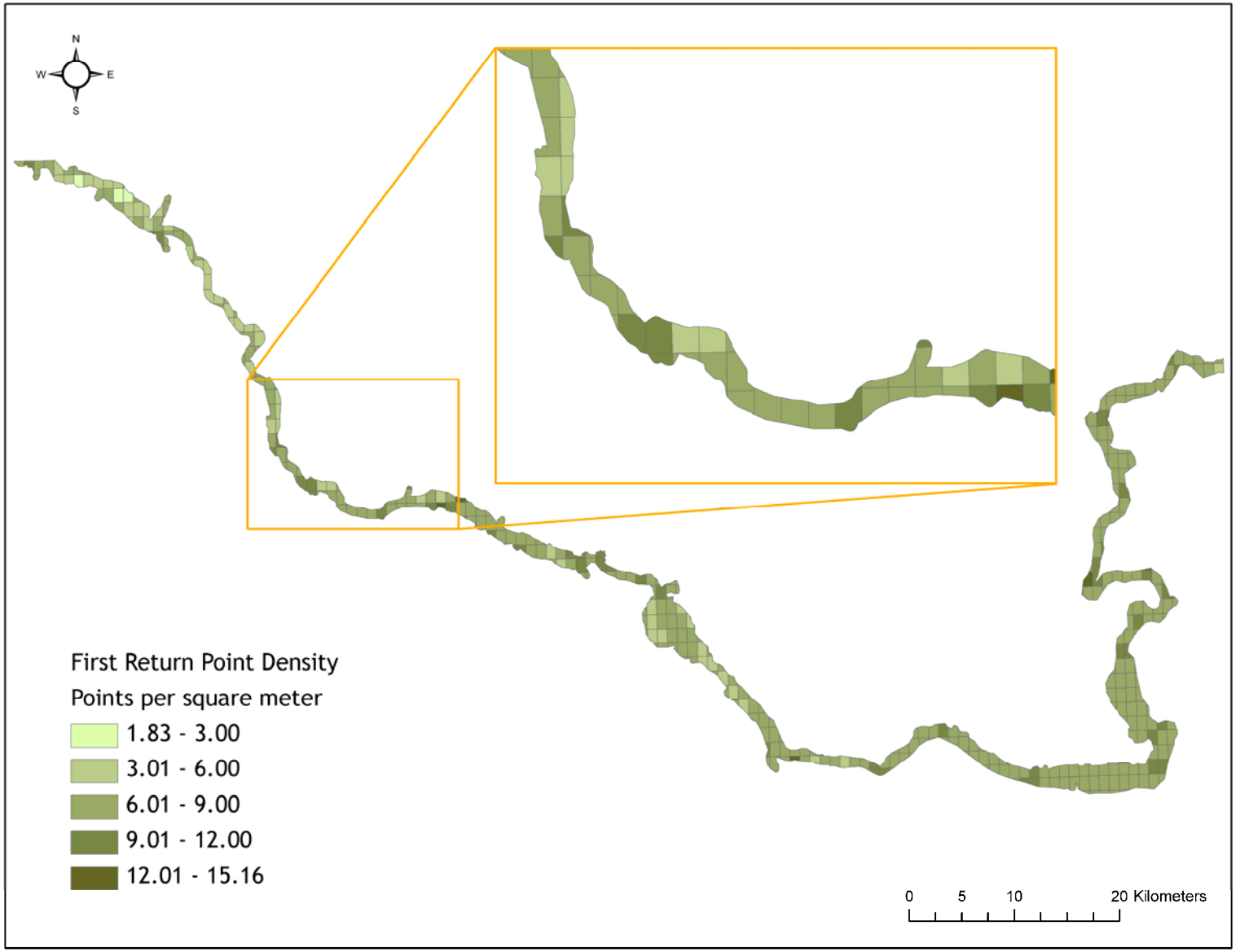

Figure 28. Delivery 10, UTM 11 density distribution map for ground classified points by USGS 0.75 minute quads.

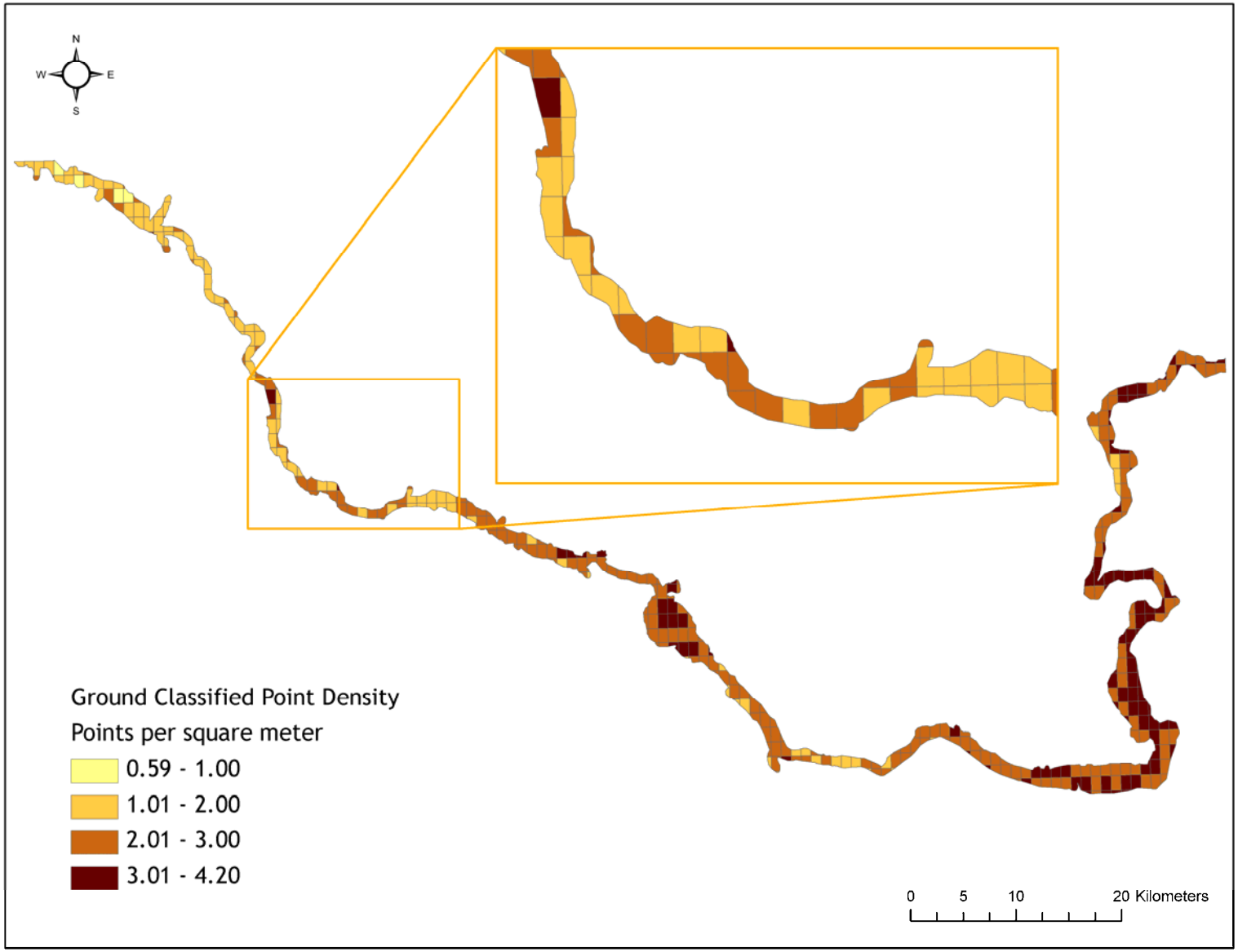

Figure 29. Delivery 11, UTM 11 density distribution map for first return points by USGS 0.75 minute quads.

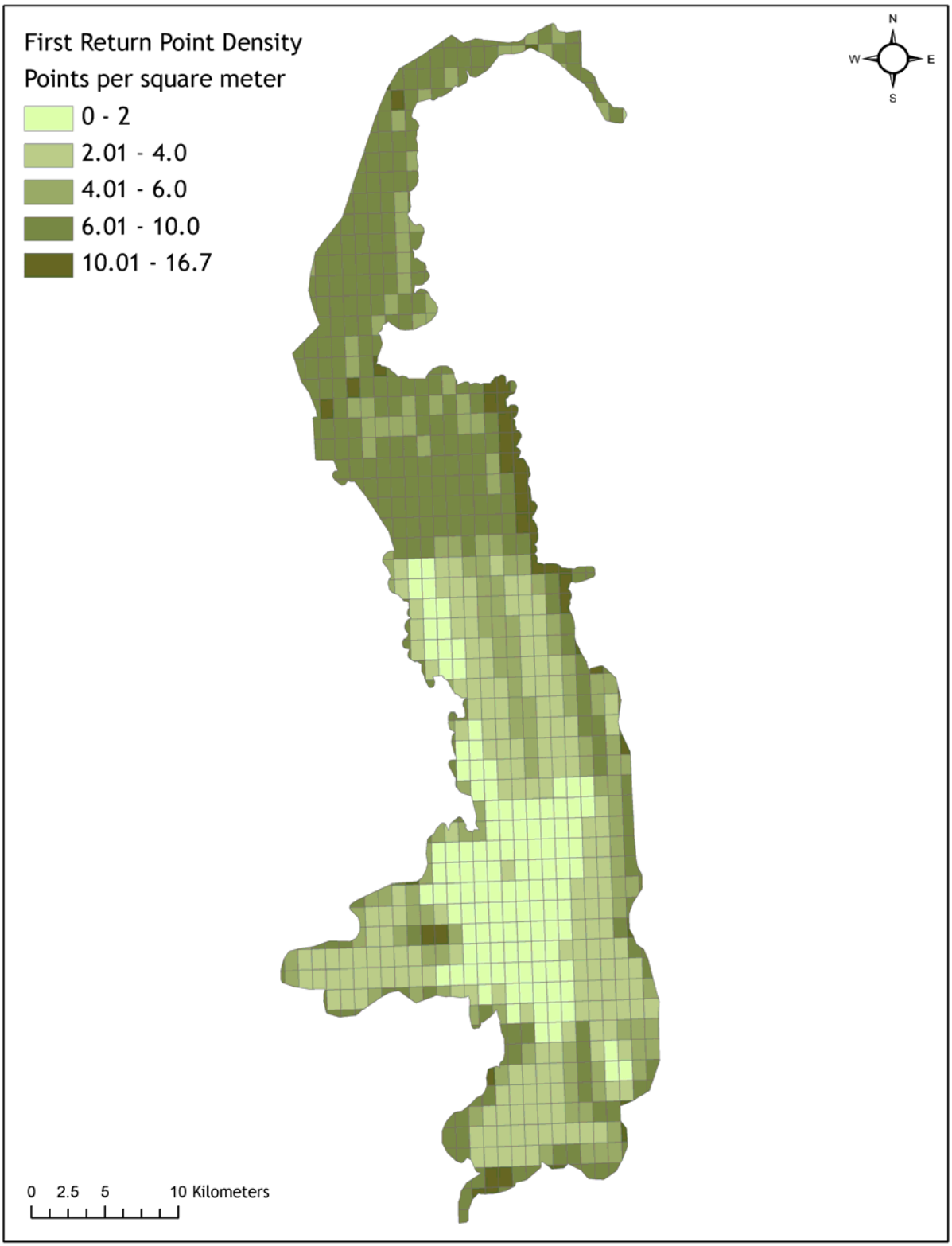

Figure 30. Delivery 11, UTM 11 density distribution map for ground classified points by USGS 0.75 minute quads.

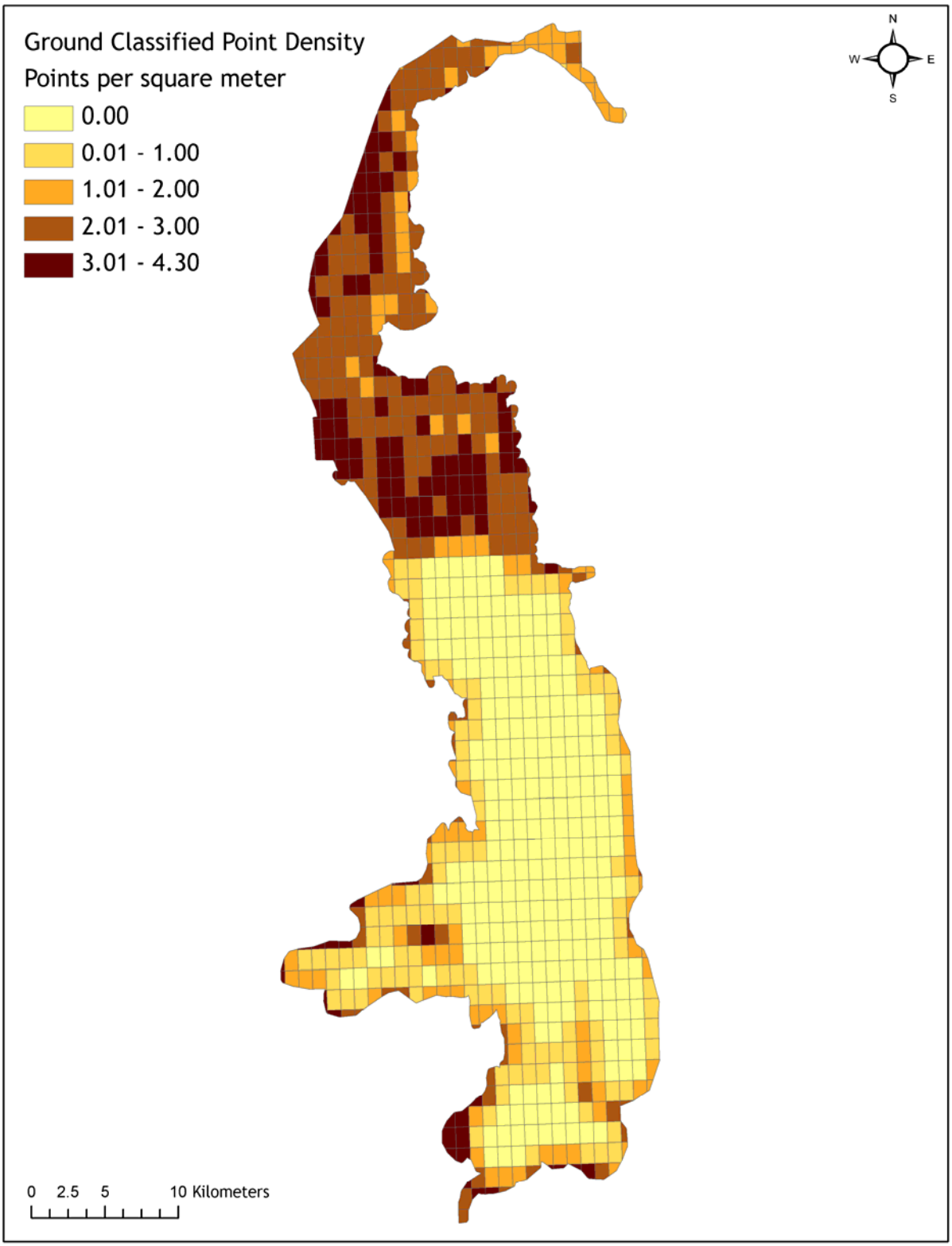

5.3 Relative Accuracy Calibration Results

Relative accuracy statistics for UTM 11 delivered to date

- Project Average = 0.041m
- Median Relative Accuracy = 0.041m
- 1σ Relative Accuracy = 0.016m
- 1.96σ Relative Accuracy = 0.032m

Figure 31. Distribution of relative accuracies per flight line, non slope-adjusted for UTM 11.

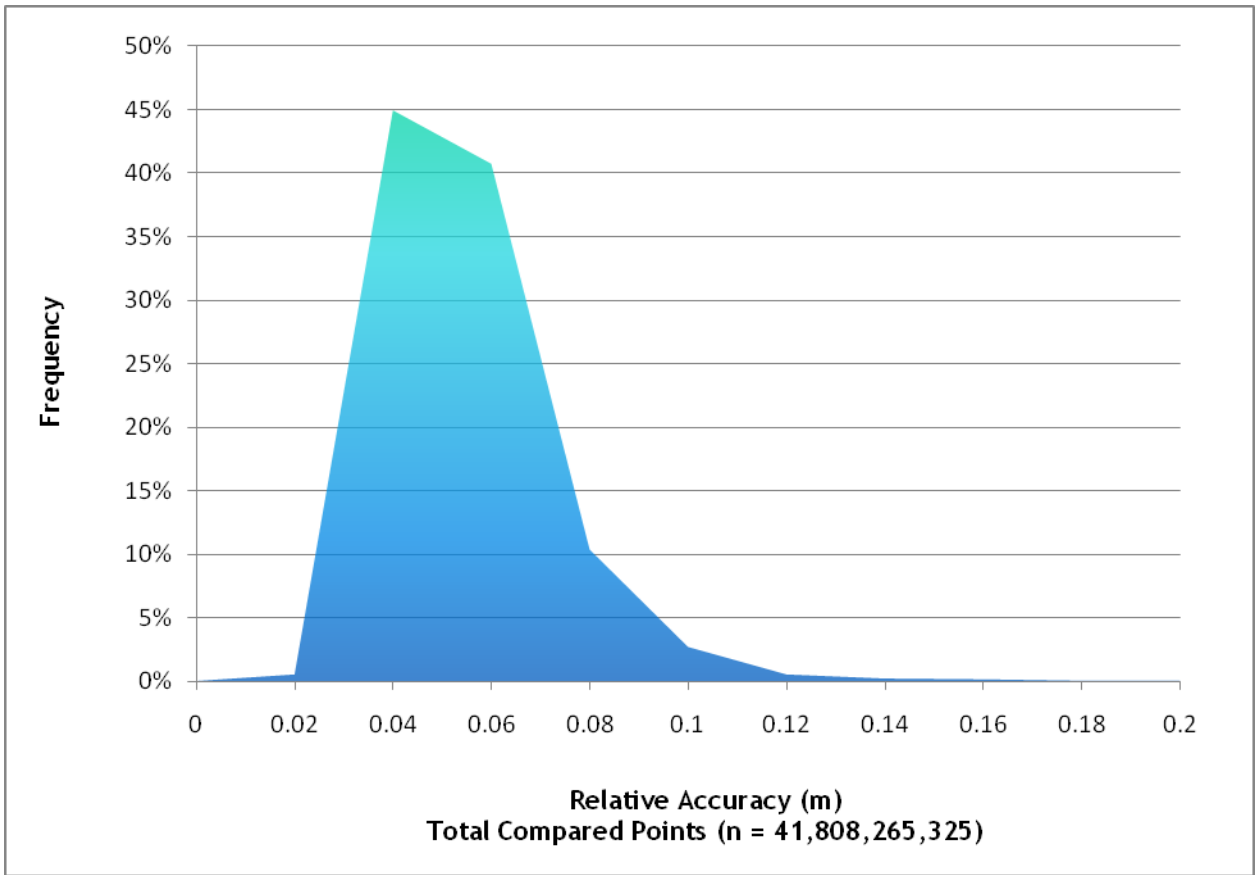

5.4 Absolute Accuracy

Table 4. Absolute Accuracy for UTM 11 – Deviation between laser points and RTK hard surface survey points.

RTK Survey Sample Size (n): 28,317	
Root Mean Square Error (RMSE) = 0.047m	Minimum Δz = -0.260m
Standard Deviations 1 sigma (σ): 0.047m 1.96 sigma (σ): 0.092m	Maximum Δz = 0.202m Average Δz = -0.005m

Figure 32. Absolute Accuracy - Histogram Statistics, based on 28,317 RTK points in UTM 11.

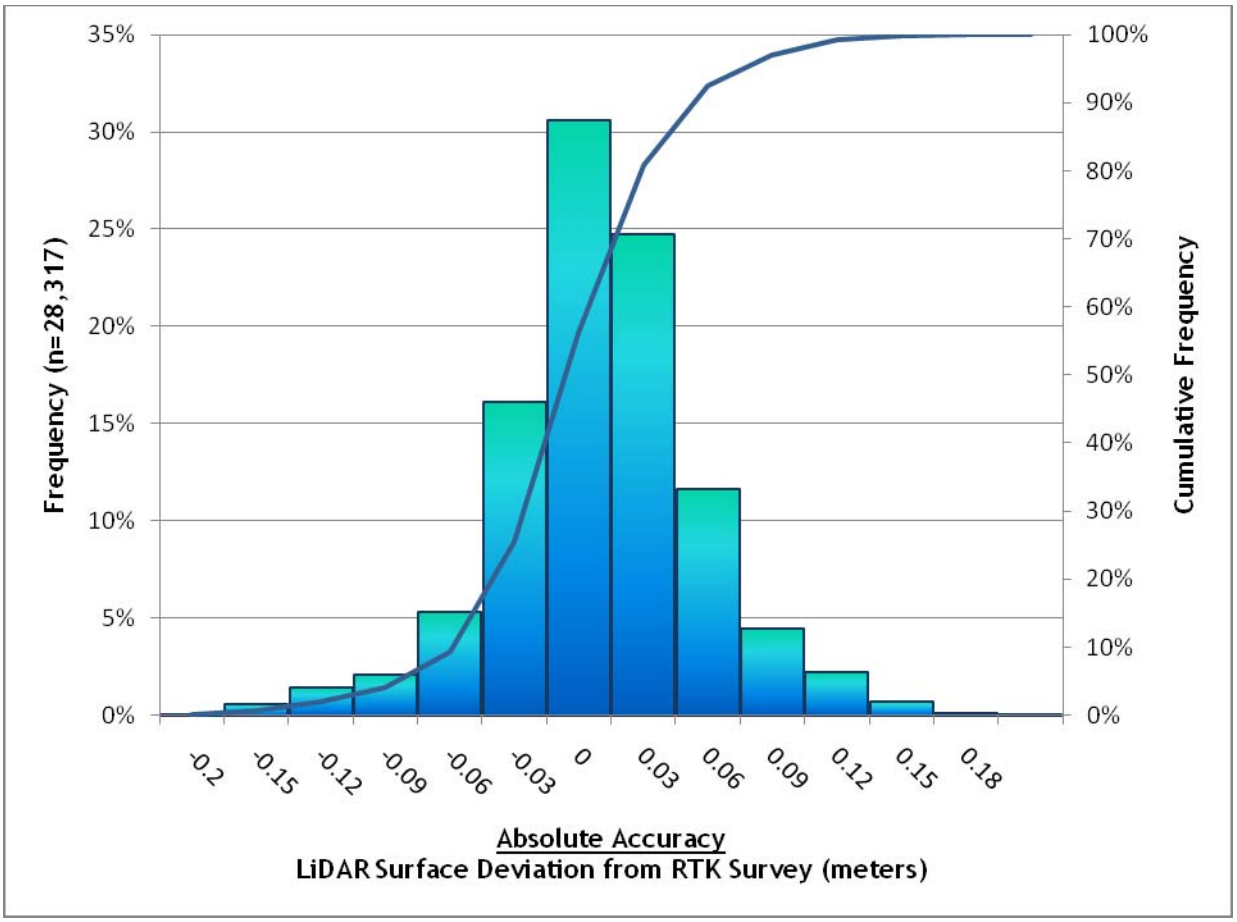

6. Breakline Enforced Terrain Model

David C. Smith and Associates (DSA) created breaklines for the Columbia River study area using LiDAR-grammetry techniques. **Table 5** describes the type and definition of each breakline collected. The breaklines were used to supplement the LiDAR data in creation of a final ground model. Water boundaries were enforced using hard breaklines and water surfaces were flattened based on the elevation from the breaklines. The breakline boundaries were also used to class any points with ground or model key point classification within the water delineated areas.

Table 5. Breaklines collected for the Columbia River study area, see Appendix B for feature definitions.

Feature	Implementation
Breakline	Hard Breakline
Breakline Obscured	Hard Breakline
Water Main	Hard Breakline
Water Island	Hard Breakline
Water Other	Hard Breakline
Buildings	Provided as Feature

7. Projection/Datum and Units

	Projection:	UTM Zone 10 and 11, NAD 83
Datum	**Vertical:**	NAVD88 Geoid09
	Horizontal:	NAD83
	Units:	meters

8. Deliverables

Point Data:	• All Returns (LAS 1.2 format)
Vector Data:	• Tile Index of LiDAR points (USGS 0.75 minute quads, shapefile) • Tile Index of DEM rasters (USGS 7.5 minute quads, shapefile) • 1-hz SBET files (shapefile) • Breaklines (dxf format) *provided by DSA* • Watermask (dxf format) *provided by DSA*

Raster Data:	• Elevation models (1 m resolution)
	  • Breakline Enforced Bare Earth Model (ESRI GRID format)
	  • Highest Hit Model (ESRI GRID format)
	• Intensity images (GeoTIFF format, 1 m resolution)

Data Report:	Full report containing introduction, methodology, and accuracy

9. Selected Images

Figure 33. 3D view looking west along Brushy Creek, the bare earth image is colored by elevation.

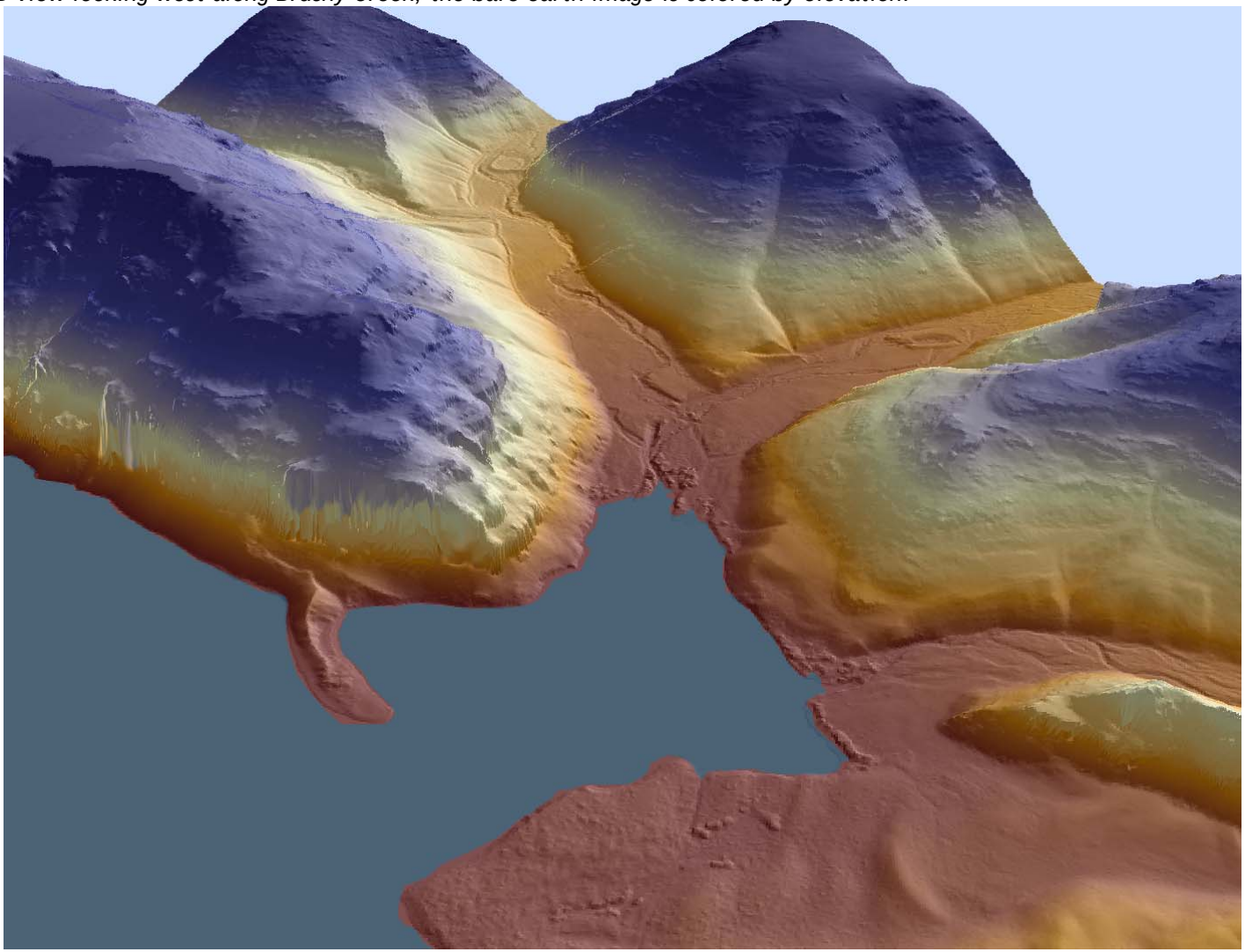

Figure 34. 3D point cloud looking north at I-5 crossing the Columbia River. MLK Blvd can be seen over I-5 and Portland Harbor is in the distance.

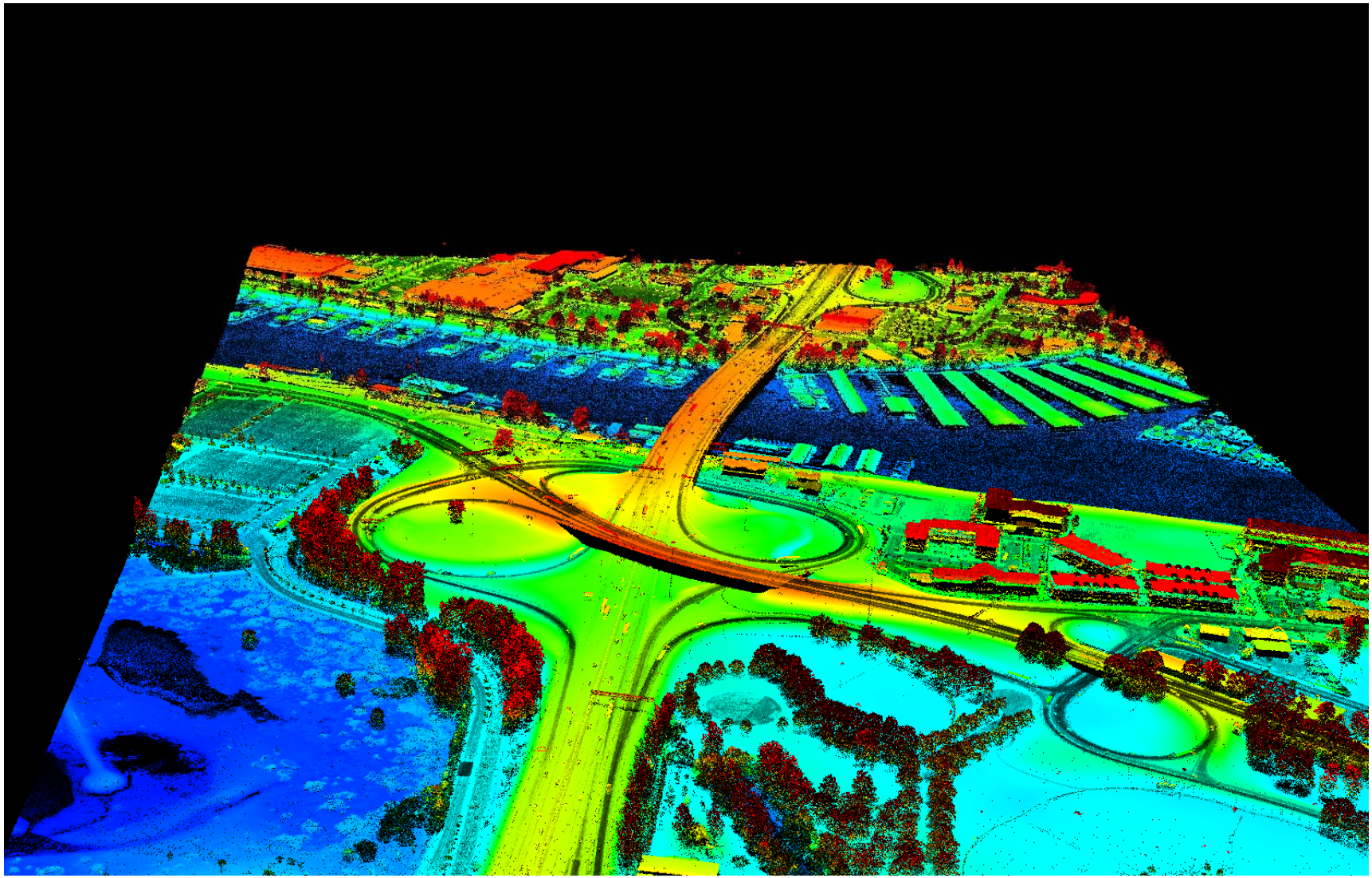

Figure 35. 3D point cloud looking southeast at middle section of Hayden island. A railroad bridge can be seen crossing the Columbia River with Portland Harbor in the far distant corner.

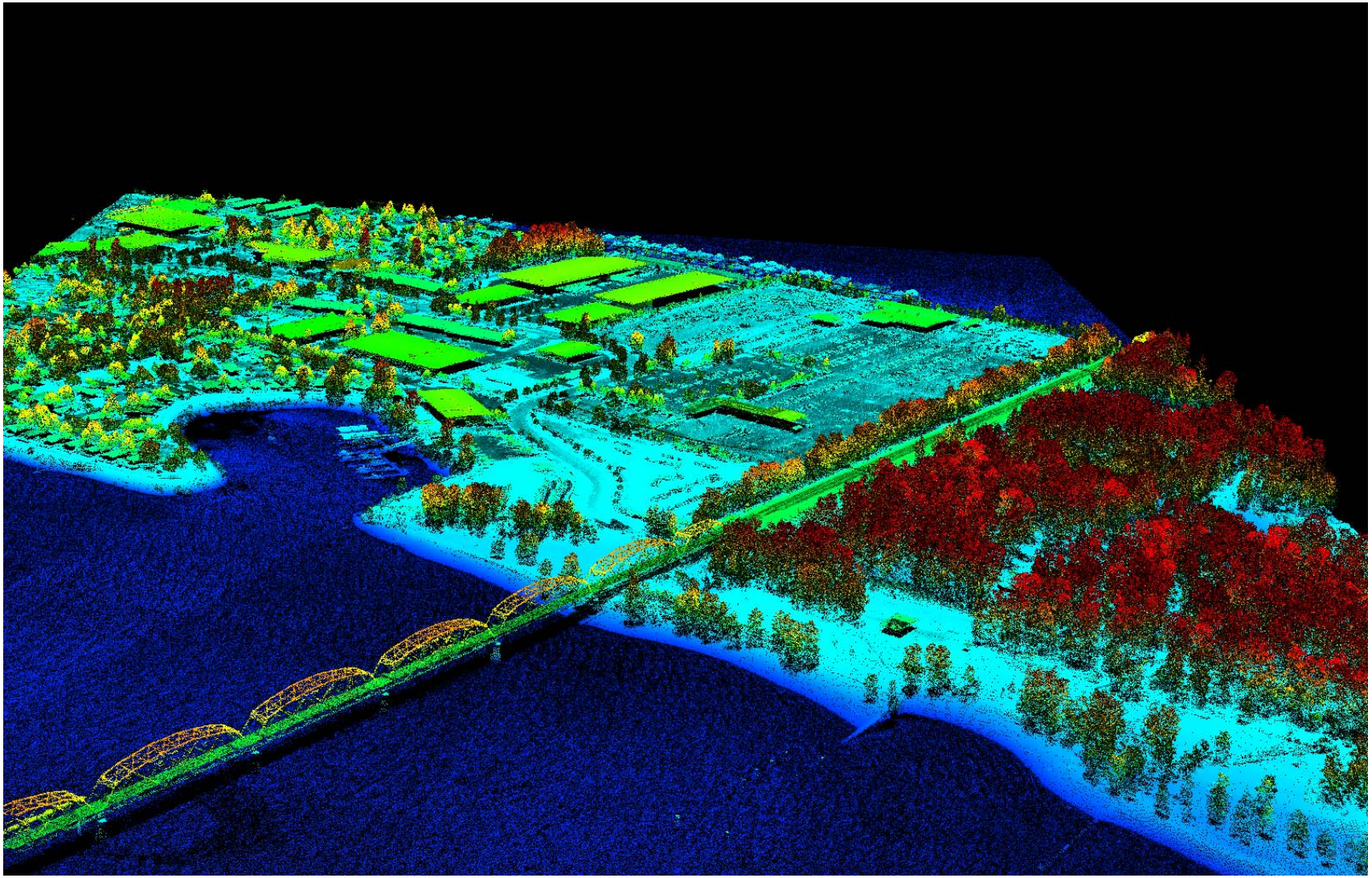

Figure 36. 3D view looking North along Longtain Creek. Top image is bare earth model colored by elevation, bottom image is NAIP draped over highest-hit model.

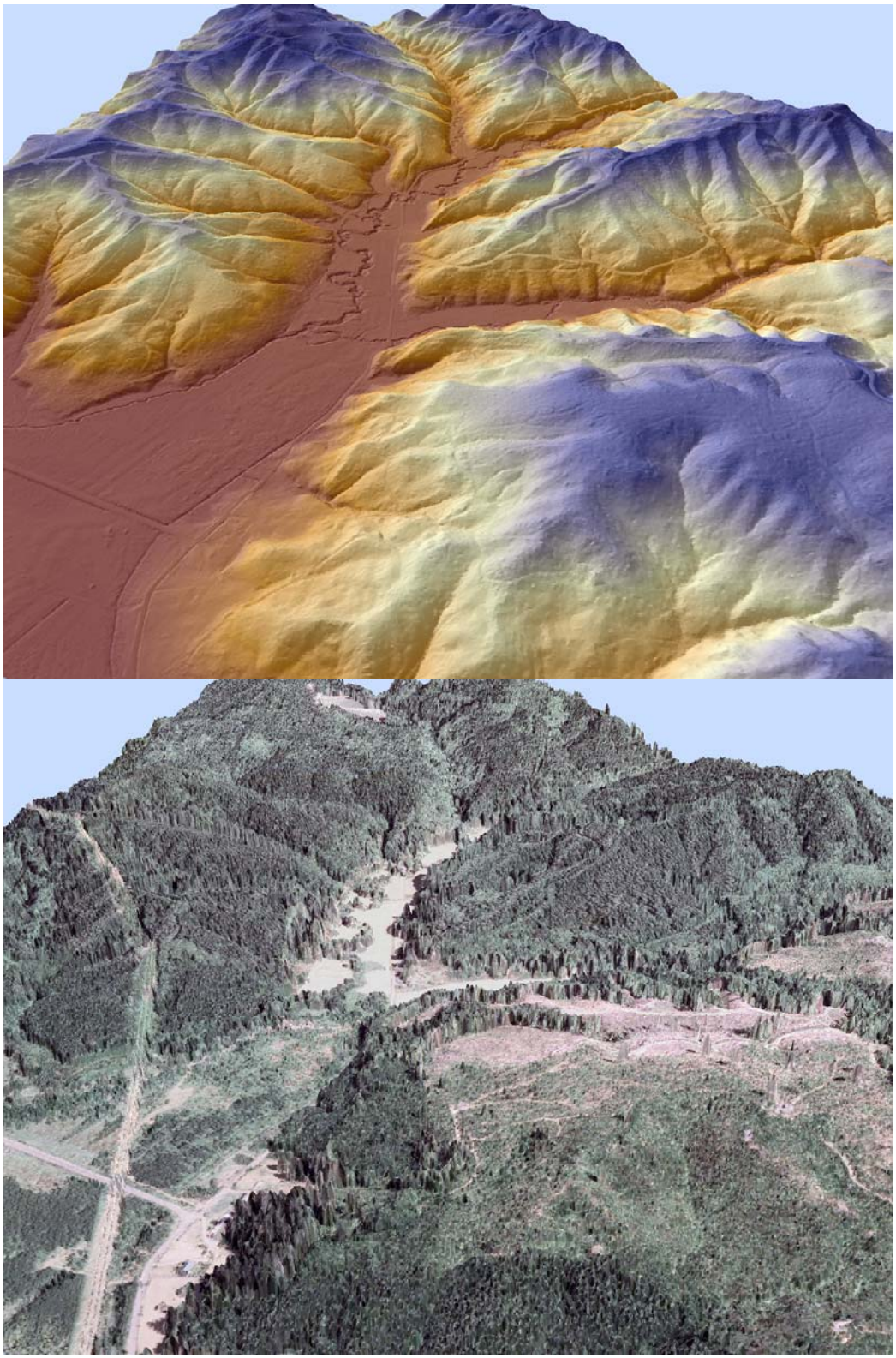

Figure 37. 3D view of West Longview looking North with Coal Creek Slough in the background. Top image is bare earth model colored by elevation, bottom image is NAIP draped over highest-hit model.

Figure 38. 3D view looking south along Franklin D Roosevelt Lake. Top image is bare earth model colored by elevation, bottom image is NAIP draped over highest-hit model.

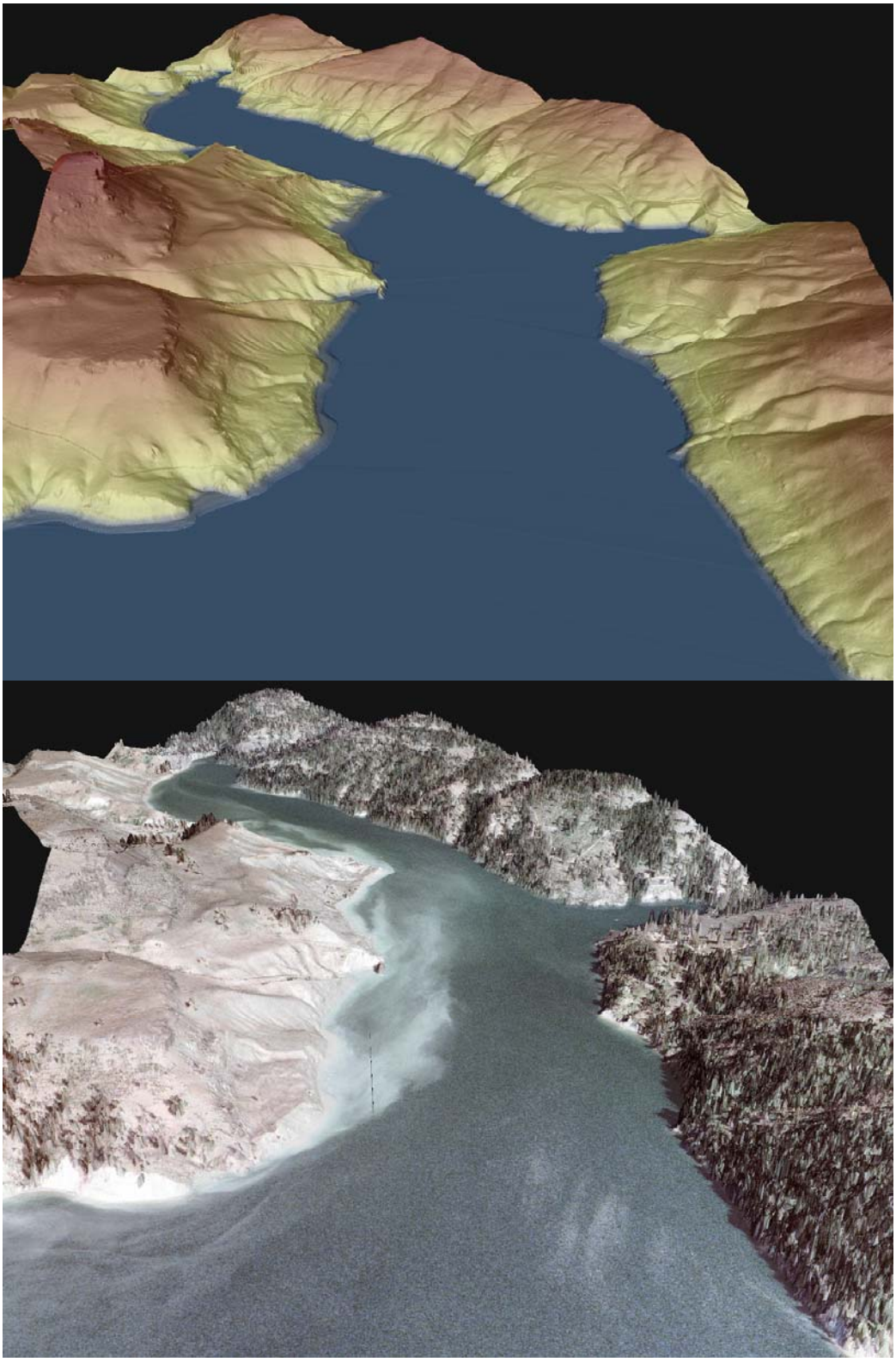

Figure 39. 3D view of Crescent Bay looking south. Top image is bare earth model colored by elevation, bottom image is NAIP draped over highest-hit model.

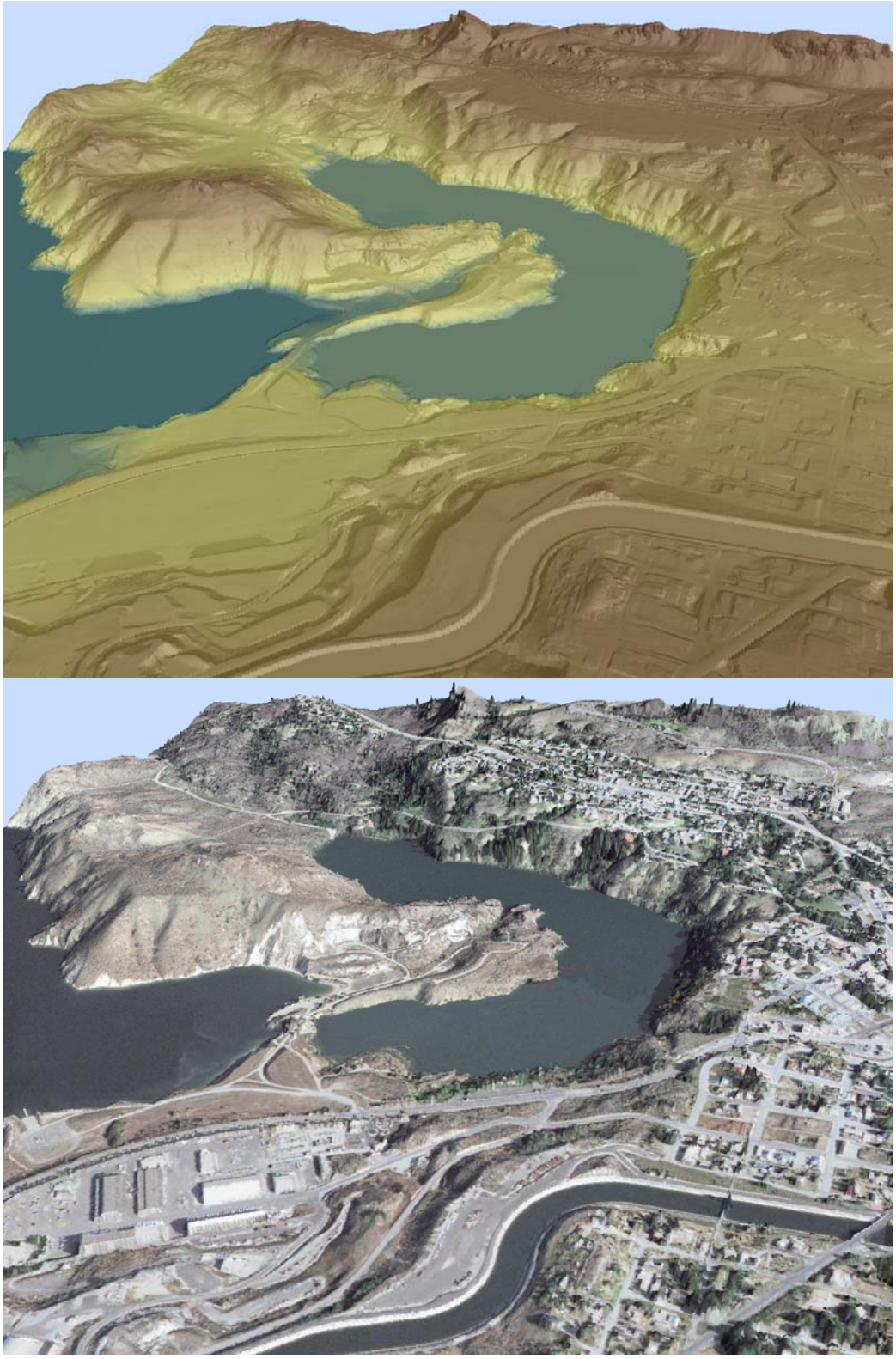

Figure 40. 3D view of Lewis and Clark Highway east of Cook, Washington along the Columbia River. Top image is bare earth model colored by elevation, bottom image is 2009 NAIP draped over highest-hit model.

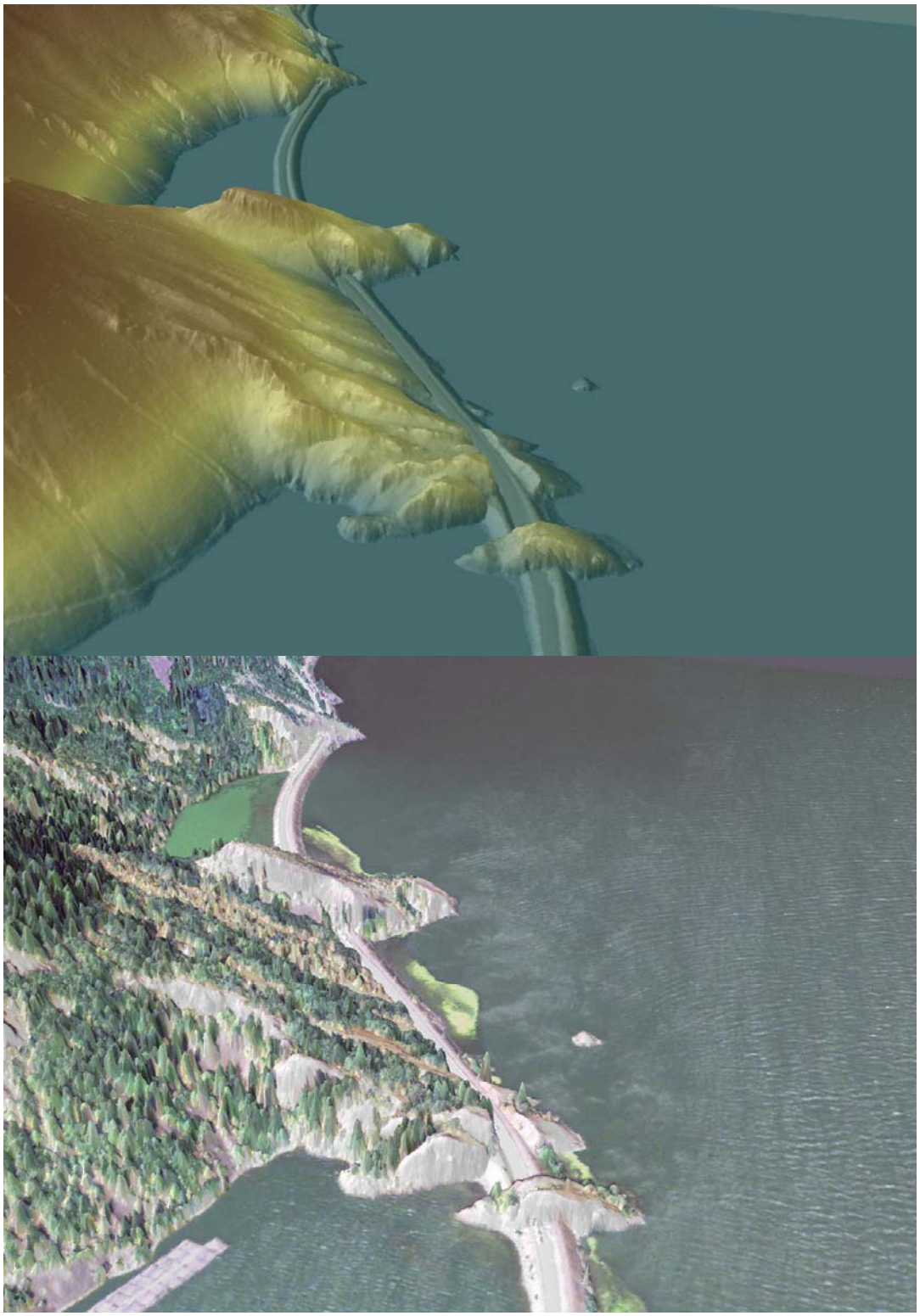

Figure 41. LiDAR point cloud colored by 2004 NAIP imagery. View looking north near Bonners Ferry, ID.

Figure 42. LiDAR point cloud colored by elevation. View looking Northwest from south of the Kootenai National Wildlife Refuge. A railroad track crosses through the scene.

Figure 43. LiDAR point cloud colored by elevation. View looking Southeast at Somers Marina in Somers, MT along Flathead Lake.

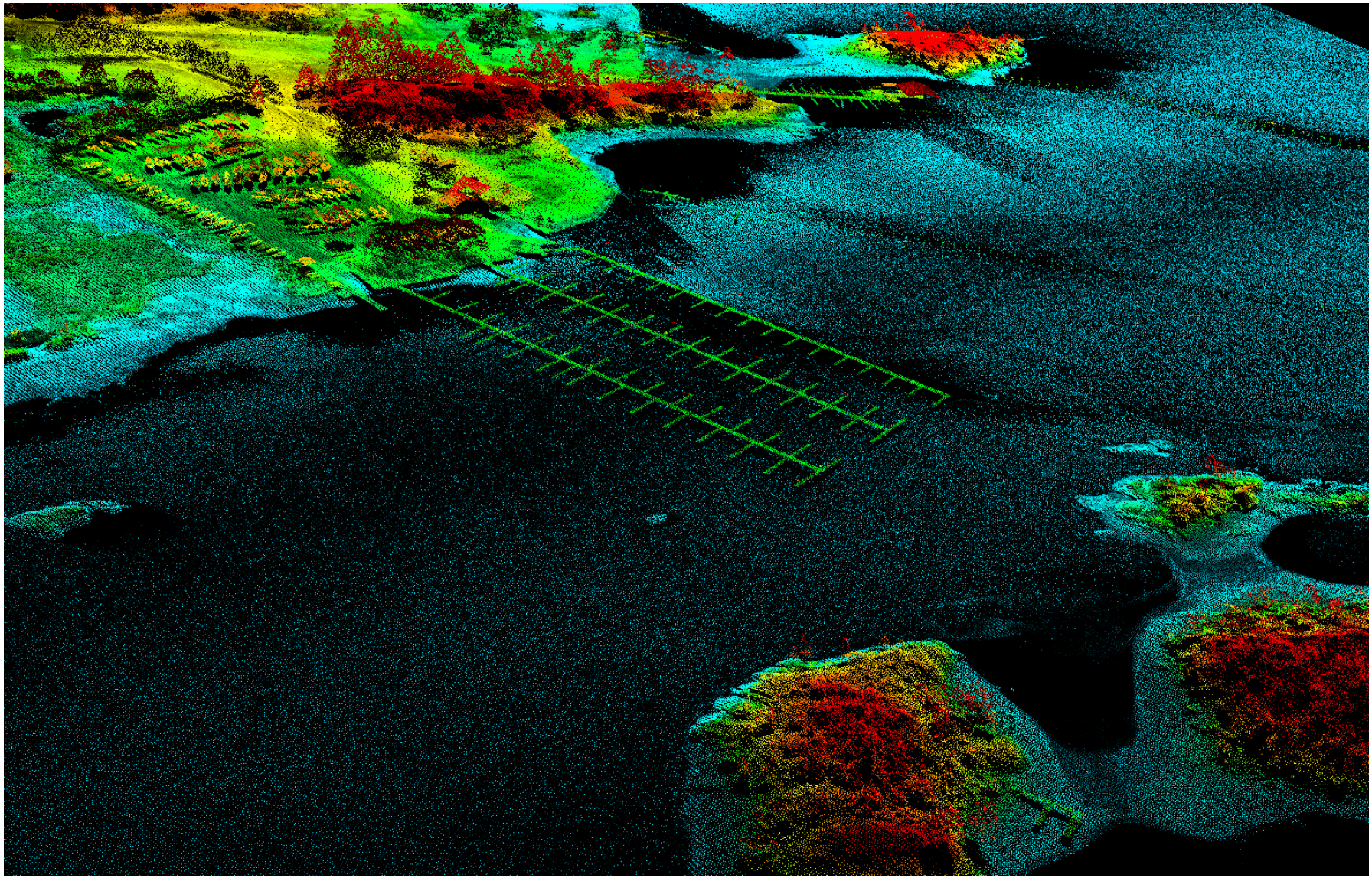

Figure 44. LiDAR point cloud colored by elevation. View looking East across Glacier Park International Airport.

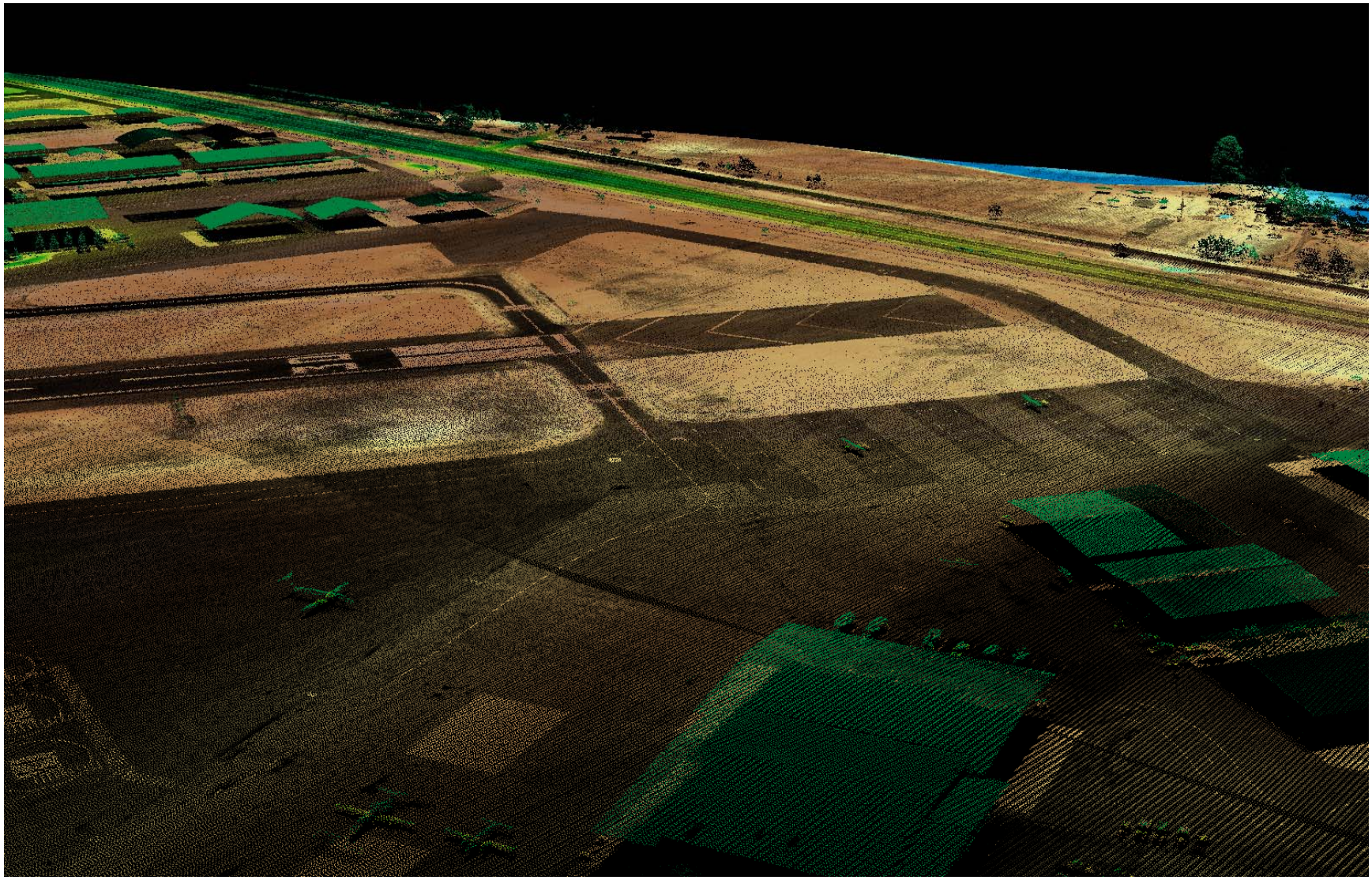

10. Glossary

1-sigma (σ) Absolute Deviation: Value for which the data are within one standard deviation (approximately 68th percentile) of a normally distributed data set.

2-sigma (σ) Absolute Deviation: Value for which the data are within two standard deviations (approximately 95th percentile) of a normally distributed data set.

Root Mean Square Error (RMSE): A statistic used to approximate the difference between real-world points and the LiDAR points. It is calculated by squaring all the values, then taking the average of the squares and taking the square root of the average.

Pulse Rate (PR): The rate at which laser pulses are emitted from the sensor; typically measured as thousands of pulses per second (kHz).

Pulse Returns: For every laser pulse emitted, the Leica ALS 50 Phase II system can record *up to four* wave forms reflected back to the sensor. Portions of the wave form that return earliest are the highest element in multi-tiered surfaces such as vegetation. Portions of the wave form that return last are the lowest element in multi-tiered surfaces.

Accuracy: The statistical comparison between known (surveyed) points and laser points. Typically measured as the standard deviation (sigma, σ) and root mean square error (RMSE).

Intensity Values: The peak power ratio of the laser return to the emitted laser. It is a function of surface reflectivity.

Data Density: A common measure of LiDAR resolution, measured as points per square meter.

Spot Spacing: Also a measure of LiDAR resolution, measured as the average distance between laser points.

Nadir: A single point or locus of points on the surface of the earth directly below a sensor as it progresses along its flight line.

Scan Angle: The angle from nadir to the edge of the scan, measured in degrees. Laser point accuracy typically decreases as scan angles increase.

Overlap: The area shared between flight lines, typically measured in percents; 100% overlap is essential to ensure complete coverage and reduce laser shadows.

DTM / DEM: These often-interchanged terms refer to models made from laser points. The digital elevation model (DEM) refers to all surfaces, including bare ground and vegetation, while the digital terrain model (DTM) refers only to those points classified as ground.

Real-Time Kinematic (RTK) Survey: GPS surveying is conducted with a GPS base station deployed over a known monument with a radio connection to a GPS rover. Both the base station and rover receive differential GPS data and the baseline correction is solved between the two. This type of ground survey is accurate to 1.5 cm or less.

11. Citations

Soininen, A. 2004. TerraScan User's Guide. TerraSolid.

Appendix A

LiDAR accuracy error sources and solutions:

Type of Error	Source	Post Processing Solution
GPS (Static/Kinematic)	Long Base Lines	None
	Poor Satellite Constellation	None
	Poor Antenna Visibility	Reduce Visibility Mask
Relative Accuracy	Poor System Calibration	Recalibrate IMU and sensor offsets/settings
	Inaccurate System	None
Laser Noise	Poor Laser Timing	None
	Poor Laser Reception	None
	Poor Laser Power	None
	Irregular Laser Shape	None

Operational measures taken to improve relative accuracy:

1. Low Flight Altitude: Terrain following is employed to maintain a constant above ground level (AGL). Laser horizontal errors are a function of flight altitude above ground (i.e., ~ 1/3000th AGL flight altitude).
2. Focus Laser Power at narrow beam footprint: A laser return must be received by the system above a power threshold to accurately record a measurement. The strength of the laser return is a function of laser emission power, laser footprint, flight altitude and the reflectivity of the target. While surface reflectivity cannot be controlled, laser power can be increased and low flight altitudes can be maintained.
3. Reduced Scan Angle: Edge-of-scan data can become inaccurate. The scan angle was reduced to a maximum of ±15° from nadir, creating a narrow swath width and greatly reducing laser shadows from trees and buildings.
4. Quality GPS: Flights took place during optimal GPS conditions (e.g., 6 or more satellites and PDOP [Position Dilution of Precision] less than 3.0). Before each flight, the PDOP was determined for the survey day. During all flight times, a dual frequency DGPS base station recording at 1–second epochs was utilized and a maximum baseline length between the aircraft and the control points was less than 19 km (11.5 miles) at all times.
5. Ground Survey: Ground survey point accuracy (i.e. <1.5 cm RMSE) occurs during optimal PDOP ranges and targets a minimal baseline distance of 4 miles between GPS rover and base. Robust statistics are, in part, a function of sample size (n) and distribution. Ground survey RTK points are distributed to the extent possible throughout multiple flight lines and across the survey area.
6. 50% Side-Lap (100% Overlap): Overlapping areas are optimized for relative accuracy testing. Laser shadowing is minimized to help increase target acquisition from multiple scan angles. Ideally, with a 50% side-lap, the most nadir portion of one flight line coincides with the edge (least nadir) portion of overlapping flight lines. A minimum of 50% side-lap with terrain-followed acquisition prevents data gaps.
7. Opposing Flight Lines: All overlapping flight lines are opposing. Pitch, roll and heading errors are amplified by a factor of two relative to the adjacent flight line(s), making misalignments easier to detect and resolve.

QA/QC Data issue responses:

An area within tile 48116F2206 was identified by DSA as a data issue. Watershed Sciences, Inc. has reviewed the LiDAR point data at this site and noted a high bridge and a steep slope. LiDAR acquisition in areas of steep terrain can create shadowing that result in low point density. Recorded flightline data indicates that acquisition was conducted according to contract specifications in this area. The lack of ground classified points represents a limitation of current LiDAR technology. However, the use of water's edge and terrain breaklines in conjunction with the LiDAR has allowed the model to interpolate through the dataset.

Figure 45. Overhead view and cross section of LiDAR point data issue in tile 48116F2206 (Kootenai River)

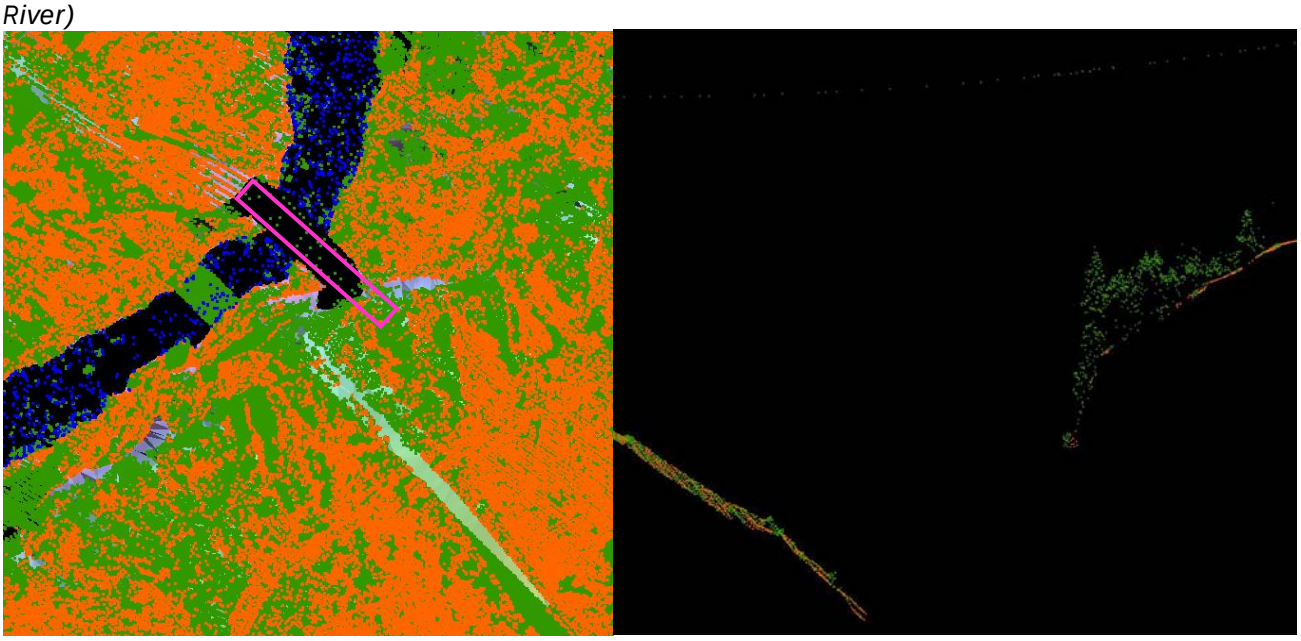

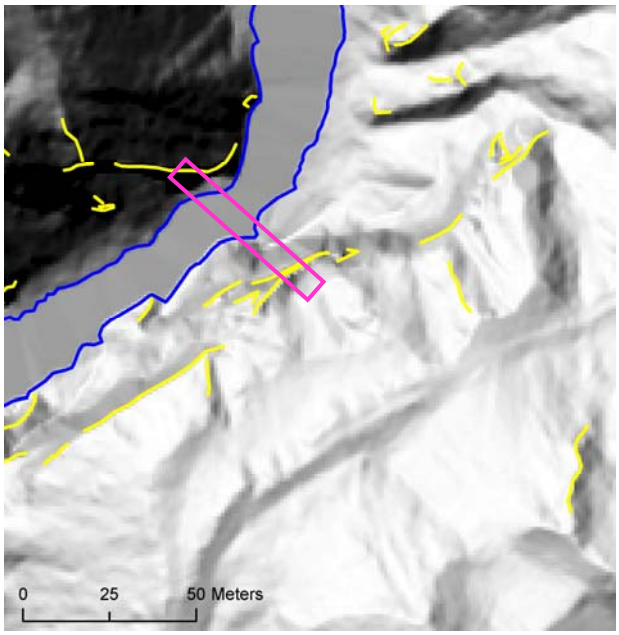

Figure 46. Resulting bare earth model with breaklines applied. Yellow lines are terrain breaks and blue lines are water breaklines.

Appendix B

Breakline definitions as determined by DSA:

FEATURE:

BREAKLINE - Added to the ground model where the LiDAR ground points were missing or not properly defining the surface. Usually occured on sharp breaks associated with cliffs. These breaks are derived from the 1st return data and fit to the ground data.

BREAKLINE_OBSCURE - Added in vegetated areas where the LiDAR ground model was not complete due to dense vegetation. These lines are interpreted from visible data and fit to visible ground data.

WATER_MAIN - Main rivers, not including side rivers and streams. Designed to be the river in the center of the coverage area, Columbia, Snake, etc.

WATER_OTHER - Covers side rivers, lakes, ponds etc. This coverage is not intended to capture all water outside the main rivers but only water edges that need a breakline and need LiDAR data re-classified. No single line streams are collected.

WATER_ISLAND - Islands in the rivers and streams.

BUILDING - Visible and obvious buildings.

BUILDING_UNSURE - Features that appear to be buildings but might not be.

BUILDING_AREA - Large areas with a dense population of buildings, subdivisions, etc.